



# Earliest life on Earth: Evidence from the Barberton Greenstone Belt, South Africa

Martin Homann

## ► To cite this version:

Martin Homann. Earliest life on Earth: Evidence from the Barberton Greenstone Belt, South Africa. Earth-Science Reviews, 2019, 196, 10.1016/j.earscirev.2019.102888 . hal-02933520

**HAL Id: hal-02933520**

**<https://hal.univ-brest.fr/hal-02933520>**

Submitted on 8 Sep 2020

**HAL** is a multi-disciplinary open access archive for the deposit and dissemination of scientific research documents, whether they are published or not. The documents may come from teaching and research institutions in France or abroad, or from public or private research centers.

L'archive ouverte pluridisciplinaire **HAL**, est destinée au dépôt et à la diffusion de documents scientifiques de niveau recherche, publiés ou non, émanant des établissements d'enseignement et de recherche français ou étrangers, des laboratoires publics ou privés.

# 1      2      3      4      5      6      7      8      9      10      11      12      13      14      15      16      17      18      19      20      21      22      23      24      25      26      27      28      29      30      31      32      33      34      35      36      37      38      39      40      41      42      43      44      45      46      47      48      49      50      51      52      53      54      55      56

1      2      3      4      5      6      7      8      9      10      11      12      13      14      15      16      17      18      19      20      21      22      23      24      25      26      27      28      29      30      31      32      33      34      35      36      37      38      39      40      41      42      43      44      45      46      47      48      49      50      51      52      53      54      55      56

1      2      3      4      5      6      7      8      9      10      11      12      13      14      15      16      17      18      19      20      21      22      23      24      25      26      27      28      29      30      31      32      33      34      35      36      37      38      39      40      41      42      43      44      45      46      47      48      49      50      51      52      53      54      55      56

1      2      3      4      5      6      7      8      9      10      11      12      13      14      15      16      17      18      19      20      21      22      23      24      25      26      27      28      29      30      31      32      33      34      35      36      37      38      39      40      41      42      43      44      45      46      47      48      49      50      51      52      53      54      55      56

1      2      3      4      5      6      7      8      9      10      11      12      13      14      15      16      17      18      19      20      21      22      23      24      25      26      27      28      29      30      31      32      33      34      35      36      37      38      39      40      41      42      43      44      45      46      47      48      49      50      51      52      53      54      55      56

1      2      3      4      5      6      7      8      9      10      11      12      13      14      15      16      17      18      19      20      21      22      23      24      25      26      27      28      29      30      31      32      33      34      35      36      37      38      39      40      41      42      43      44      45      46      47      48      49      50      51      52      53      54      55      56

## 1. Introduction

The Archean rock record is sparse, largely metamorphosed, and preserved in fragmented Greenstone Belts, which occur wedged in between plutonic and metamorphic rocks in the cratonic lithosphere of nearly all continents. However, only the Barberton Greenstone Belt (BGB) of South Africa and Swaziland and the contemporaneous Pilbara Greenstone Belts (PGBs) of Western Australia contain well-preserved sedimentary rocks of Paleoproterozoic age ( $>3.2$  Ga), which experienced only greenschist facies metamorphism and relatively minor deformation. With an area of  $\sim 6000$  km<sup>2</sup> and an age of  $\sim 3.55$ – $3.20$  Ga the BGB is significantly smaller and captures a slightly shorter time interval in comparison to the PGBs ( $\sim 60000$  km<sup>2</sup>,  $\sim 3.52$ – $2.94$  Ga), however, the deposits preserved in the BGB are characterized by often laterally consistent outcrops with correlatable facies, a generally better exposure, and very good accessibility. Lithified aquatic sediments in both of these volcano-sedimentary “enclaves” are considered the most suitable archive of ancient microbial life, as water is one of the fundamental requirements for life. Consequently, the sedimentary deposits have been extensively studied for traces of early life in these two localities and the reported findings have been critically reviewed especially for the Pilbara Greenstone Belts, where stromatolites, microfossils, and isotopic signals belong to the most dominant biosignatures (e.g. Allwood et al., 2006; Brasier et al., 2006; Wacey, 2009, 2012). The focus of this study here is to summarize and review the South African evidence of Paleoproterozoic life reported from the BGB, place them in a consistent stratigraphic framework, and discuss and evaluate the most recent findings.

## 2. Geology of the BGB

The Barberton Greenstone Belt of South Africa and Swaziland is located at the eastern margin of the Kaapvaal Craton and contains volcanic, shallow intrusive, and sedimentary rocks, ranging in age from  $<3.547$  to  $>3.219$  Ga (Byerly et al., 2019; Fig. 1). These age constraints are mainly derived from high-precision zircon U-Pb age dating of interbedded volcanic units and plutons surrounding the BGB, as well as detrital zircon geochronology. Rocks of the Barberton Supergroup (formerly named Swaziland Supergroup), are subdivided from base to top into three lithostratigraphic units: (1) the  $\sim 8$ – $10$  km thick, volcanic-dominated Onverwacht Group, which comprises the Komati, Hooggenoeg, Kromberg, and Mendon Formations (Viljoen and Viljoen, 1969; Anhaeusser, 1976; Lowe and Byerly, 2007; De Wit and Furnes, H., 2011); (2) the up to  $\sim 2$  km thick Fig Tree Group, predominantly composed of interlayered volcanoclastic strata that mark the final stages of major volcanism and the transition to deposition of terrigenous clastic units (Heinrichs and Reimer, 1977; Lowe, 1999a; Hofmann, 2005; Byerly et al., 2019); and (3) the up to  $3.5$  km thick, coarse-grained siliciclastic to conglomeritic Moodies Group, mainly derived

from the erosion of underlying units and uplifted plutonic rocks (Eriksson, 1977; Heubeck and Lowe, 1994a, 1994b, 1999). The dominant large-scale orogeny of the BGB occurred contemporaneously with deposition of the Moodies Group at 3.225–3.215 Ga (Lamb and Paris, 1988; Heubeck et al., 2013). Although the BGB strata experienced several phases of major deformation during which they were folded, faulted and altered, the rocks are generally well-preserved in locally very thick and laterally-traceable sections (De Ronde and De Wit, 1994; Toulkeridis et al., 1998; Lowe and Byerly, 1999). A major fault system, the Inyoka Fault, transects the BGB approximately medially and divides it into a northern and southern facies, characterized by distinct differences in the preserved stratigraphy and depositional facies of especially the Onverwacht and Fig Tree Groups (Fig. 2). Although approximately coeval, these deposits represent previously geographically separated successions that are now in tectonic contact with another (Byerly et al., 2019). The greenstone belt fill can be further subdivided into several tectonostratigraphic blocks, each bordered by numerous, steeply dipping large and small faults (Lowe, 1999a; Lowe et al., 2012). Most rocks in the central part of the BGB experienced alteration temperatures of >300°C (Xie et al., 1997; Toulkeridis et al., 1998; Tice et al., 2004), however some primary mineralogy, textures, and sedimentary structures have been preserved in many units due to the combination of early silicification and the local partitioning of strain (Byerly et al., 2019).

### 3. History of early life studies in the BGB

The BGB has a long history of studies focusing on traces of early life and the reconstruction of its habitat, metabolism, biogeochemical cycling, and mode of preservation (Table 1). Since the mid-1960s the occurrence of lenticular, spheroidal, and filamentous microstructures, interpreted as possible cellular microfossils, has been reported from carbonaceous cherts of the Onverwacht Group\* (Barghoorn and Schopf, 1966; Pflug, 1966, 1967; Schopf and Barghoorn, 1967; Pflug et al., 1969; Barghoorn, 1971). \*[Note that these samples were collected from the same outcrop, which was originally assigned to the Fig Tree Group, but later revised and changed to the upper Onverwacht Group (Pflug, 1967; Schopf, 1975; Lowe and Knauth, 1977).] In the following years simple spherical and filamentous microstructures have also been described from other Onverwacht Group cherts of the Mendon and Kromberg Formation (Engel et al., 1968; Nagy and Nagy, 1969; Brooks and Shaw, 1971; Brooks et al., 1973; Muir and Hall, 1974; Muir and Grant, 1976; Knoll and Barghoorn, 1977), however the exact stratigraphic position was often not clearly indicated, which made it challenging to put the individual findings in context to each other. In fact, the insufficient knowledge of the BGB stratigraphy at that time and the often poorly studied depositional facies, and paleoenvironmental context of the analyzed samples are central problems of most of these pioneering studies. Due to their often simply morphology and wide size range the biogenicity of almost all of the early-



reported microfossils has been questioned in several reviews (Schopf, 1975; Schopf and Walter, 1983; Altermann, 2001; Wacey, 2009), which suggested that except for the structures described by Muir and Grant (1976) and Knoll and Barghoorn (1977) all other findings should be treated as nonfossil artefacts, aggregates of amorphous carbonaceous matter or modern contaminants. More detailed sedimentological, geochronological, and tectonostratigraphic investigations of the BGB deposits (Lowe and Knauth, 1977; Kröner et al., 1991; Lowe and Byerly, 1999; Lowe et al., 2012), organic carbon isotope analysis (e.g. Oehler et al., 1972), the identification of possible stromatolites (de Wit et al., 1982; Byerly et al., 1986; Byerly and Palmer, 1991; Walsh, 2004), and new discoveries of mat-like laminations, lenticular, spheroidal, and filamentous microfossil in cherts of the Hooggenoeg, Kromberg, and Mendon Formations (Walsh and Lowe, 1985, 1999; Walsh, 1992; Westall et al., 2001; Glikson et al., 2008) supported previous findings (e.g. Pflug, 1966; Knoll and Barghoorn, 1977) and stimulated further investigations. In the following, carbonaceous laminations preserved in the shallow-water facies of the Buck Reef Chert (Kromberg Formation) have been studied in great detail and were interpreted as the remains of photosynthetic microbial mats (Tice and Lowe, 2004, 2006a, 2006b; Tice, 2009; Tice et al., 2011). Westall et al. (2006, 2011, 2015, 2018) identified microbial biofilms and possible fossil bacteria in the Josefsdal Chert (Kromberg Formation) and suggested that these microbial communities were once thriving in a nearshore hydrothermal setting. Tubular, titanite-mineralized microstructures in basaltic pillow lava rims of the Hooggenoeg and Kromberg Formations were interpreted as being the result of microbial etching, and thus indicating the presence of submarine thermophilic microbial communities during basalt formation (Furnes, 2004; Banerjee et al., 2007; Furnes et al., 2007; Fliegel et al., 2010). However, the syngenicity and biogenicity of these putative oldest trace fossils has been strongly questioned and is currently still under debate (McLoughlin et al., 2012; Grosch and McLoughlin, 2014; Staudigel et al., 2015; Wacey et al., 2017; Hickman-Lewis et al., 2019 for a short review). More recently, the biogenicity of lenticular microfossils from the Kromberg Formation was further supported by *in situ* carbon isotope analysis (Oehler et al., 2017), while new findings of cell-like objects from the Buck Reef Chert were interpreted as degraded colonies of coccoidal bacteria (Kremer and Kaźmierczak, 2017). Moreover, Hickman-Lewis et al. (2018) reported carbonaceous laminations, resembling microbial biofilms and mats from the Middle Marker at the base of the Hooggenoeg Formation, making it to the most ancient claim for life in the BGB.

In the last decade also the sand- and siltstones of Moodies Group (uppermost unit of the BGB), were carefully investigated for traces of early microbial life, which resulted in the discovery of large spheroidal microfossils (Javaux et al., 2010), widespread shallow-marine tufted microbial mats once formed by photosynthetic microorganisms (Noffke et al., 2006; Heubeck, 2009; Gamper et al., 2012; Homann et al., 2015) and remnants of cavity-dwelling microbial communities (Homann et al., 2016). Terrestrial microbial mats interbedded with fluvial sandstones and conglomerates, record a significant difference in their organic

carbon and nitrogen isotopes in comparison with the tidal marine mats and represent the oldest macroscopically-visible trace of life on land (Homann et al., 2018). The presence of a Paleoproterozoic terrestrial biosphere is further supported by the Moodies Group paleosols that carry signals of biogenic sulfur fractionation (Nabhan et al., 2016a, 2016b). In the following, a selection of the most promising and best documented claims for early life from the Onverwacht and Moodies Groups of the BGB will be described and discussed in more detail.

#### 4. The 3.55–3.26 Onverwacht Group

The Onverwacht Group consists of a up to 10 km thick succession of mostly of mafic and ultramafic volcanic rocks with minor felsic volcanic flow units and tuffs (Lowe and Byerly, 1999). Subordinate sedimentary units formed during episodic breaks in eruptive activity and have been widely silicified to bedded cherts, which host a large number of the reported traces of early life in the BGB, including microbial mats, microfossils, and possible stromatolites. Moreover, rare asteroid ejecta layers, composed of impact spherules, fine ash and dust, locally occur as discrete beds and record distal impact events of large asteroids with diameters ranging between 20–50 km (Fig. 2; Lowe and Byerly, 1986, 2018). The Onverwacht Group comprises four different formations (Komati, Hooggenoeg, Kromberg, and Mendon), which each can be further subdivided into informal members (e.g. H1 - H6). Within each member the cherts, which are capping individual volcanic units are designated with a "c" (e.g. H4c; Lowe and Byerly, 1999; Byerly et al., 2019). Overlying the basal Komati Formation, the 3.472 - 3.416 Ga Hooggenoeg Formation consists of thick sequence of tholeiitic basalts, minor komatiites, and thin chert units and can reach a thickness of up to 3900 m on the western limb of the Onverwacht Anticline (Viljoen and Viljoen, 1969b, Lowe and Byerly, 1999). The 3.416 – 3.334 Ga Kromberg Formation on the west limb of the Onverwacht Anticline comprises an up to 1800-m-thick succession of black and banded chert (Buck Reef Chert, K1), mafic lapilli tuff and lapillistone (K2), and tholeiitic basalt (K3), while on the eastern limb of the anticline massive pillow basalt is more abundant. The top of the formation is marked by a regionally traceable chert unit, the Footbridge Chert (K3c; Viljoen and Viljoen, 1969, Lowe and Byerly, 1999). Conformably overlying the Kromberg Formation, the 3.334 – 3.258 Ga Mendon Formation has a thickness of >600m and records an alternation of volcanic cycles, each characterized by a komatiitic flow unit capped by a chert layer (Byerly, 1999).

##### 4.1 Microbial mats

The first systematic stratigraphic and petrographic analysis of all carbonaceous cherts in the Hooggenoeg, Kromberg, and Mendon Formation of the Onverwacht Group was made by Walsh (1992) and Walsh and Lowe (1999), who distinguished three main types: black-and-white banded, massive black, and black laminated chert. The carbonaceous matter in these cherts occurs mostly in the form of: fine laminations (1

– 20 µm thick), carbonaceous wisps (10–50 µm thick, 50–1000 µm long) that are likely eroded fragments of the fine laminations, subrounded composite grains (100–1000 µm), and irregular-shaped simple grains (5–750 µm), and. Based on bulk  $\delta^{13}\text{C}_{\text{org}}$  values ranging between –40.8‰ and –16.9‰, with a mean of –29.8‰ (n = 50), Walsh and Lowe (1999) concluded that all the carbonaceous matter in the cherts is probably of biological origin, which was further supported by a detailed study of van Zuilen et al. (2007), combining Raman spectroscopy and SIMS (secondary ion mass spectrometry) analysis.

In detail, the fine carbonaceous laminations that form layers of 0.5–2 cm thickness and occur predominantly in black-and-white banded cherts the Hooggenoeg (H2, H4c, H5c), Kromberg (K1, K3c), and Mendon Formation (M1c, M2c), were interpreted as remains of microbial mats (Walsh, 1992; Walsh and Lowe, 1999; Trower and Lowe, 2016). The alternation of carbonaceous black bands with thin layers of pure (white) quartz in these cherts is likely comparable with alternating organic-rich and organic-poor sediments in modern microbial mats. The mats presumably formed in periods of volcanic quiescence but likely under the presence of hydrothermal activity. They are often interbedded with layers of composite carbonaceous grains, which Walsh (1992) compared to globular bacterial colonies or organic aggregates, however, the biogenicity of these grains still needs to be further established (Trower and Lowe, 2016). In the following, reported microbial mats and biofilms from the Middle Marker, the Buck Reef Chert, and Josefsdal Chert will be described in more detail.

#### 4.1.1 Middle Marker

The 3.472 Ga Middle Marker (H1) at the base of the Hooggenoeg Formation represents the oldest, relatively unmetamorphosed sedimentary unit of the BGB (Lanier and Lowe, 1982; Armstrong et al., 1990). It has a thickness of 3 to 6 m and is composed of silicified komatiitic ash and fine layers of relatively pure carbonaceous cherts that contain composite grains and carbonaceous wisps of proposed biogenic origin (Lanier and Lowe, 1982; Walsh, 1992; Lowe, 1999; Walsh and Lowe, 1999). Deposition occurred likely on a flat, tide- or wave influenced shelf in water depths of several 10s to 100 m (Byerly et al., 2019).

Fine, crinkly laminations, interbedded with the volcanoclastic sand- and siltstones of this unit, have been interpreted as fossil microbial mats by Hickman-Lewis et al. (2018), mainly based on their carbonaceous composition, micro-tufted morphology, sediment trapping and cohesive behavior, and the occurrence of wisp-like structures, interpreted as erosional mat (Fig. 3A and B). The carbonaceous laminations occur in packets of 200 µm to 2.5 mm thickness, contain detrital quartz and volcanic grains, and generally have a low surficial relief, which is described by the authors as micro-tufted (Fig. 3A and B). These crinkly, micro-tufted structures (<100µm in height) of proposed primary biogenic origin can be distinguished from pseudo-tufted structures (up to 0.8 mm in height) that formed secondary as a result of plastic deformation triggered by the settling of dense particles (Fig. 3C and D; Hickman-Lewis et al., 2018). The micro-tufted structures

337  
338  
339 206 were further used by Hickman-Lewis et al., (2018) to tenta  
340 207 were formed by anoxygenic phototrophs. However, it is hard to constrain the microbial metabolism relying  
341  
342 208 on mat morphology alone, especially if it is only of minor topographic relief and secondary deformation  
343 209 structures are present. More valuable insights into the metabolism(s) of the Middle Marker mats could be  
344  
345 210 gained from the analysis of organic carbon isotopes, which would also help to further strengthen their  
346 211 biogenicity.  
347  
348 212

#### 349 213 **4.1.2 Buck Reef Chert**

350 214 The 3.416 Ga Buck Reef Chert (K1) is a 250–400-m-thick unit of carbonaceous and ferruginous cherts at  
351  
352 215 the base of the Kromberg Formation, exposed continuously along nearly 50 km of strike in the west limb  
353 216 of the Onverwacht Anticline (Kröner et al., 1991; Lowe and Worrell, 1999). A correlative section in the  
354  
355 217 east limb of the Onverwacht Anticline comprises three 10–25-m-thick chert units (Kc1, Kc2, Kc3), that are  
356 218 interbedded with basalt flows (Walsh, 1992; Lowe and Byerly, 1999). The cherts are thought to be of  
357  
358 219 primary origin and likely precipitated from normal marine water, which was saturated with respect to  
359 220 amorphous silica during the Archean (Lowe, 1999b; Knauth and Lowe, 2003; Tice and Lowe, 2006a) rather  
360  
361 221 than from hydrothermal fluids (de Wit et al., 1982; Westall et al., 2001). Sediments of the Buck Reef Chert  
362 222 were deposited on subsiding open-marine volcanic platform and can be subdivided in three main  
363 223 depositional facies (basal evaporitic, middle platform, and deep basin), which reflect deposition under  
364  
365 224 successively deeper-water conditions (Tice and Lowe, 2004). The silicified evaporites from the evaporitic  
366 225 facies, were originally interpreted as remnants of nahcolite (Lowe and Worrell, 1999) but may represent  
367  
368 226 pseudomorphs after aragonite (Otálora et al., 2018). Fine anastomosing carbonaceous laminations (Fig. 4A-  
369 227 F) and in places ripped up, plastically deformed rolled-up fragments (Fig. 5 A and B), occurring within  
370  
371 228 black bands in black-and-white banded cherts of the platform facies, were interpreted as remnants of  
372 229 cohesive microbial mats (Walsh and Lowe, 1999; Tice and Lowe, 2004, 2006a, 2006b; Tice, 2009; Tice et  
373  
374 230 al., 2011). The mats were once thriving in shallow-water, photic zone paleoenvironments below fair-  
375  
376 231 weather wave base and show three distinct mat morphotypes: (1) alpha-type, fine carbonaceous laminations  
377 232 that incorporate and loosely drape detrital grains underlying detrital grains and form silica-filled lenses (Fig.  
378  
379 233 4A and B); (2) beta-type, fine meshworks of filament-like strands (<5µm in diameter), which drape  
380 234 underlying detrital grains (Fig. 4C and D); and (3) gamma-type, evenly spaced flat laminations that tightly  
381  
382 235 drape underlying sediments (Fig. 4E and F; Tice, 2009). The formation of different mat morphotypes is  
383 236 thought to be primarily controlled by local variations in ambient light intensity and/or current energy.  
384 237 Consequently, the first two morphotypes (alpha and beta) probably formed in shallower water, which is  
385  
386 238 also supported by their more complex morphology and association with coarser-grained sediments (Tice  
387 239 2009). Bulk organic carbon isotope measurements of the carbonaceous laminations, with  $\delta^{13}\text{C}_{\text{org}}$  values  
388  
389  
390  
391  
392

ranging between  $-36.9\text{‰}$  and  $-20.1\text{‰}$ , and a mean of  $-29.9\text{‰}$  ( $n = 19$ , Tice and Lowe 2006b), serve as additional evidence for a biogenic origin of the mats, which were formed by photosynthetic microbes that most likely applied hydrogen-based carbon fixation (Tice and Lowe, 2004a, 2006a). Raman microspectroscopic analysis further revealed that the carbonaceous matter preserved in the Buck Reef Chert has experienced sub- to lower-greenschist facies temperatures, consistent with regional peak metamorphic temperatures, and thus confirming its syngenetic origin (Tice et al., 2004; van Zuilen et al., 2007). Overall, the microbial mats preserved in the Buck Reef Chert represent one of the best documented evidence for ancient life in the Onverwacht Group. Future work could focus more on micro-scale investigations, increase the spatial resolution of organic carbon isotope measurements, and try to acquire also nitrogen isotope values in order to learn more about the biogeochemical cycling of these elements by the mat-forming microbial communities.

#### **4.1.3 Josefsdal Chert**

The Josefsdal Chert comprises a 6–30-m-thick succession of silicified volcanoclastic rocks, located in a fault-bounded sliver, and is considered to be the lateral equivalent of the 3.334 Ga Footbridge Chert (K3c; (Kröner et al., 1996; Lowe and Byerly, 1999) at the top of the Kromberg Formation (Hofmann and Bolhar, 2007; Westall et al., 2015). Sedimentary structures, such as ripple marks, planar- and cross-lamination indicate that deposition likely occurred in tidal, nearshore environments under the influence of hydrothermal activity, which is supported by REE patterns with positive Eu and Y anomalies and was likely driven by the circulation of silica-saturated seawater through cooling basaltic lavas that occur stratigraphically below the Josefsdal Chert (Hofmann and Harris, 2008; Westall et al., 2011, 2015, 2018). Cracks, only a few  $\mu\text{m}$  in width, occurring in structures interpreted as fossil biofilms from these deposits, were further used to infer periods of subaerial exposure, desiccation, and evaporation (Westall et al., 2001; 2006). Such cracks are, however, less suitable to reconstruct the depositional context, as they are only visible with the SEM (scanning electron microscope) and not in the outcrops. Altermann (2001) suggested that these cracks and the pseudomorphic evaporite minerals, as well as some putative rod-shaped microfossils (2–3.8 mm long and interpreted as remnants of sulphate-reducing bacteria) described by Westall et al. (2001, 2006) from these cherts, might represent sample preparation artefacts introduced during HF etching (Wacey, 2009). Moreover, the fact that the anions of the putative, often idiomorphic, evaporite crystals have been replaced by fluorine (Westall et al., 2006) further indicates that they could represent artefacts, especially as it has been shown that mineral artefacts such as fluorides and fluosilicates commonly form during HF etching (Karkhanis, 1977) and might mimic evaporitic minerals. A more promising candidate for life in these deposits are therefore the structures that are visible in petrographic

thin section and resemble silicified biofilms and microbial mats (Fig 6 A-C). The microbial mat-like structures occur in banded black and white cherts as layered packets, 100–1000  $\mu\text{m}$  thick, that are composed of  $\sim 10\mu\text{m}$  thin, wavy carbonaceous biofilms with incorporated fine-grained detrital volcanic clasts and quartz grains (Westall et al., 2006; 2011; 2015). Torn and plastically deformed fragments of these biofilms occur partially peeled off below and above distinct mat horizons, which is interpreted as evidence for contemporaneous (lateral?) injection of hydrothermal fluids (Fig. 6D, Westall et al., 2015). A single biofilm (1–4  $\mu\text{m}$  thick) exposed on fresh fractured bedding surface has been extensively studied by Westall et al. (2001, 2006, 2011; sample 96SA05) and SEM observations revealed the presence of multiple layers of parallel filament-like structures with constant diameter of 0.25  $\mu\text{m}$ , which are embedded in a granular to smooth film interpreted as extracellular polymeric substance. Carbonaceous clots, 50–500  $\mu\text{m}$  in diameter and interpreted as degraded remnants of chemosynthetic biomass, represent another proposed biosignature from Josefsdal Chert (Westall et al., 2015), however their biogenicity still needs to be further established. Two bulk organic carbon isotope measurements from the Josefsdal Chert show  $\delta^{13}\text{C}_{\text{org}}$  values of  $-22.7\text{‰}$  (bulk sample, Westall, et al 2001) and  $-26.8\text{‰}$  (carbon-rich black layer, Westall et al., 2006). While *in situ* measurements of the carbonaceous biofilms yield  $\delta^{13}\text{C}_{\text{org}}$  values of  $-45\text{‰}$  to  $-13\text{‰}$  and a single  $\delta^{34}\text{S}$  value of  $-24\text{‰}$  (Westall et al., 2015). These values support a biogenic origin of the biofilms/mats and were further used to conclude that the latter were formed by anoxygenic photosynthesizers and sulphur reducing bacteria (Westall et al. 2011, 2015). Future *in situ* isotope studies on the organic remains in these samples should increase the amount of data points and aim to better document the analytical areas (see e.g. Williford et al. 2013, 2016) in order to spatially resolve the large range of  $\delta^{13}\text{C}_{\text{org}}$  values, and to distinguish it from the background signal of the carbonaceous cherts, which might differ significantly, as documented by Oehler et al. (2017) for samples of the Buck Reef Chert that show  $\delta^{13}\text{C}_{\text{org}}$  values ranging between  $-47.1\text{‰}$  and  $-24.0\text{‰}$ .

## 4.2 Microfossils

The positive identification of Archean microfossils is due to their often very simple morphology extremely challenging, several well-established criteria exist (see Schopf, 2004; Brasier et al., 2006; Wacey, 2009), while *in situ* carbon isotope analysis of individual microfossil candidates has become another required method for the evaluation of their biogenicity in recent years (e.g. House et al., 2013; Lepot et al., 2013; Williford et al., 2013, 2016). Putative microfossils in the carbonaceous cherts of the Onverwacht Group are extremely rare. The first systematic analysis of Walsh (1992) and Walsh and Lowe (1999) revealed that only 9 of more than 400 analyzed samples contained possible microfossils of filamentous, lenticular, and spheroidal shapes.

#### 4.2.1 Filamentous structures

Filamentous microstructures of carbonaceous composition were identified in a single 2 cm thick black-and-white banded chert layer in the upper Hooggenoeg Formation (Walsh and Lowe, 1985; Walsh 1992). These tread-like or cylindrical, unbranched filaments are solid, 0.2 – 2.5 µm in diameter, up to 200 µm long and occur associated with carbonaceous laminations interpreted as microbial mats. Although originally classified as possible microfossils Walsh (2000) noted that they may have formed abiotically and could thus represent simple mineral filaments (Wacey, 2009).

More convincingly biological filaments occur associated with fossil mats in several localities of the Buck Reef Chert (K1 and K1c2; Byerly et al., 2019). The hollow cylindrical filaments, 1.2 – 1.4 µm in diameter and 10 – 150 µm in length, are composed of carbonaceous matter and fine pyrite (Fig. 7A-C). They mostly occur oriented subparallel to bedding or sometimes as interwoven, tangled clumps (Walsh and Lowe, 1985; Walsh 1992). These hollow, sheath-like filaments are similar in size and shape to modern filamentous bacteria and are of possible organic origin (Walsh 1992, Altermann, 2001), however, high-resolution petrographic and detailed *in situ* carbon isotope analysis would be desirable to further support this interpretation.

#### 4.2.2 Lenticular structures

Lenticular structures (previously named “spindle-shaped” structures) represent a group of enigmatic microfossils that are also well-known from the Pilbara Craton of Western Australia where their biogenicity is well established (e.g. Sugitani et al., 2007, 2010, 2013, Oehler et al., 2009, 2017; House et al., 2013; Kozawa et al., 2018). There, the lenticular objects occur individually or in groups or chains of several individuals. Lense- or, disk-shaped microstructures, 30–60 µm in long axis, with hollow centers and carbonaceous walls have been first documented in the BGB by Pflug (1966, 1967) and Pflug et al., (1969) from cherts of the Fig Tree Group that were later assigned to the upper Onverwacht Group (Mendon Formation, previously named Swartkoppie Formation, (Schopf, 1975; Lowe and Knauth, 1977)). The structures gently taper towards the ends of their long axes, occur isolated or sometimes in groups of two or more specimens (Fig. 8A-D), which are connected at their poles, and were interpreted as the remains of thread-like bacterial colonies (Pflug, 1966, 1967). Walsh (1992) interpreted very similar lenticular structures, 13–135 µm long and 4.5–61 µm wide, from detrital layers above the basal evaporitic facies of the Buck Reef Chert (K1) as possible sheaths of colonies of bacterial cells or carbonaceous coatings around former gypsum crystals (Fig. 8E-H). A biological origin of the structures is supported by *in situ*  $\delta^{13}\text{C}_{\text{org}}$  analysis that revealed values ranging between -39.3‰ to - 35.5 ‰, consistent with autotrophic carbon fixation (n = 8; Oehler et al., 2017). Based on their robust morphology, shallow water habitat and  $\delta^{13}\text{C}_{\text{org}}$

values Oehler et al. (2017) proposed that the lenticular forms might represent microbes with a planktonic stage in their life cycle, making it to a very promising claim for microbial life in the BGB.

#### 4.2.3 Spheroidal structures

Spheroidal microstructures of carbonaceous composition belong to a very common group of putative microfossils in the Onverwacht Group but the evaluation of their biogenicity is due to their simple morphology often very challenging.

Glikson et al. (2008) identified clusters of spheroidal, cell-like objects (2–10  $\mu\text{m}$  in diameter) with granular walls from cherts of the Hooggenoeg Formation (H3c and H5c), which display features of possible cell wall degradation (Fig. 9A and B). The spheroids are comparable with the modern hyperthermophilic *Methanocaldococcus jannaschii* and were thus interpreted as remnants of chemosynthetic microbes once thriving in a seafloor hydrothermal system. This is a promising sign for life, but follow-up studies should also document the sedimentological context, perform analysis on more than two samples, and include *in situ* isotope measurements (Wacey et al., 2009). Large granular-walled spheroids and ellipsoids (10–84  $\mu\text{m}$  in length; Fig. 9C and D) and clusters of thin-walled spheroids (4.5–12.8  $\mu\text{m}$  in diameter; Fig. 9E and F) from the Buck Reef Chert were interpreted as probable microfossils of coccoidal bacteria or spores (Walsh, 1992). However, these simple spheres may be produced abiotically in various ways and were therefore reinterpreted as abiotic self-organized structures, such as spherulitic chert (Brasier et al., 2006). Kremer and Kazmierczak (2017) reported spheroidal microstructures, 3–12  $\mu\text{m}$  in diameter, from the Buck Reef Chert (K1c2) and tentatively conclude that they may represent the variably degraded remains of coccoidal cyanobacteria (Fig. 9G and H). Although the cell-like objects occur in groups or clusters, preserved in black cherts with bulk  $\delta^{13}\text{C}_{\text{org}}$  values of  $-26.5\text{‰}$  and  $-24.3\text{‰}$  ( $n = 2$ ), their outer walls often have a more angular than rounded appearance, which resemble crystal terminations, thus making a biological origin less favorable (Hickman-Lewis, 2019). Alternatively, these objects might represent carbonaceous linings on replaced minerals or crystal rims (Brasier et al., 2006). Moreover, beyond morphological similarity, the positive identification of cyanobacteria and oxygenic photosynthesis hundreds of millions of years before most other evidence, requires independent geochemical evidence for the local presence of free oxygen, which is currently not available. Future studies should include nanoscale analysis of the putative cell walls and *in situ* isotope measurements.

Another occurrence of possible organic microspheres, 1–4  $\mu\text{m}$  in diameter, has been described by Knoll and Barghoorn (1977) from the Msauli Chert (M1c; Mendon Formation, previously named Swartkoppie Formation (Lowe, 1999c)), which was deposited in shallow-water nearshore environments (Fig. 9I). These carbonaceous spheres occur as isolated or paired objects, are often flatten, wrinkled or folded, show a narrow unimodal size frequency distribution ( $n = 200$ ), evidence of possible cell division, and were



interpreted as the remains of primitive prokaryotes (Knoll and Barghoorn, 1977). However, without any geochemical analysis also these structures cannot be unambiguously identified as biological (Wacey, 2009).

### 4.3 Stromatolites

Compared to its Australian counterpart the currently known stromatolite occurrences in the BGB are very rare. Byerly et al. (1986) reported putative pseudocolumnar stromatolites that crop out for more than 10 km along strike in grey to black cherts assigned to member M2c of the ~3.23 Ga Mendon Formation (Walsh, 2004; Lowe and Byerly, 2015), which is interbedded with komatiitic lava flow deposits. [Note that these outcrops were initially assigned to the Fig Tree Group (Byerly et al., 1986), but are now thought to belong to the Mendon Formation in the upper Onverwacht Group (Lowe, 1994)]. The possible stromatolites occur in layers of <1 to 20 cm thickness and display variable morphologies, ranging between low-relief, asymmetrical, sometimes laterally-linked domes (1–3 cm wide and 0.5–3 cm high), rare pseudocolumns with bridging laminae (up to 10 cm height), and crinkly stratiform laminations (50–100 µm thick; Fig. 10A and B). Individual laminae are composed of minor amounts of primary carbonaceous matter and variable amounts of secondary, fine-grained, often idiomorphic tourmaline minerals (sometimes up to 50%), which may have been derived through the hydrothermal remobilization of previously formed, boron-rich evaporites (Fig. 10C; Byerly and Palmer, 1991). Alternatively, the tourmaline mineralization could have been caused by heating and partial ocean evaporation related to a large asteroid impact recorded by spherule beds S5 and S8, which occur associated with some of the stromatolites (Lowe and Byerly, 2015). Conglomerates composed of laminated silica chips occur in the throughs between stromatolite domes and have been interpreted as fragments of eroded stromatolites or sinter crusts, likely deposited in the aftermath of a large impact (Fig. 10D). Similar stromatolite-crust chip conglomerates have also been reported from the Fig Tree Group (Sheba Formation) where they are overlain by spherule bed S5 (Lowe and Byerly, 2015, 2018). The stromatolitic structures were possibly formed by hyperthermophilic microbial communities in shallow-water depositional environments during periods of relative volcanic quiescence and likely experienced the profound effect of distant asteroid impacts (Byerly et al., 1986; Lowe and Byerly, 2018). The widespread occurrence, morphological variability, and similarity to other fossil and modern stromatolites suggest a biogenic origin of these structures (Awramik, 1992). However, organic carbon isotope measurements, three-dimensional morphological investigations, a better documentation of the different morphotypes (Allwood et al., 2006), combined with high-resolution petrographic analysis, and a clear distinction from possibly abiogenic hot-spring silica crust precipitates (Lowe, 1994) would be desirable to further support this interpretation.

410

## 5. The ~3.22 Ga Moodies Group

The ca. 3.22 Ga Moodies Group is the uppermost stratigraphic unit of the BGB and represents the world's oldest well-preserved alluvial to shallow-marine tidal deposit. It consists of a up to 3.5 km thick succession of quartz-rich sandstones with subordinate conglomerates, mudstones, siltstones, thin volcanic tuff beds, minor banded iron formations and a basaltic lava, deposited in marine (deltaic, inter-, and subtidal) and terrestrial (alluvial, fluvial, possibly aeolian) paleoenvironments (Hall, 1918; Visser, 1956; Anhaeusser, 1976; Eriksson, 1977, 1979, Heubeck and Lowe, 1994a, 1999; Simpson et al., 2012; Homann et al., 2015, 2018; Heubeck et al., 2016). The age of the Moodies Group is tightly constrained by Uranium–lead dating of single-zircons from several dacitic tuffs and rare felsic dykes, which indicate that deposition began about  $3.223 \pm 1$  Ga and had ended by about  $3.219 \pm 9$  Ga (De Ronde and Kamo, 2000; Heubeck et al., 2013). Moodies strata north of the Inyoka Fault are preserved in several, commonly northward-overtuned synclines that are tectonically separated by major faults (Fig. 2). These deposits not only contain a large variety of well- preserved sedimentary structures, they also offer a high-resolution archive of Paleoarchean surface and sedimentation processes, as well as a unique window into a widespread, diverse and well adapted microbial ecosystem. Reported biosignatures from the Moodies Group include intertidal and fluvial microbial mats, silicified remnants of cavity-dwelling microorganisms (coelobionts), and large organic-walled microfossils (acritarchs), as detailed below.

### 5.1 Microbial mats

Fossil microbial mats in the Moodies Group have been identified so far in intertidal deposits of the Saddleback Syncline and in alluvial-fluvial deposits of the Dycedale Syncline (Fig. 11A-C). In the Saddleback Syncline the mats are preserved as carbonaceous, crinkly laminations (0.5–1 mm thick), interbedded with medium- to coarse-grained sandstones, and associated with desiccation cracks (Fig. 12A) They represent the oldest known examples of siliciclastic tidal mats in the geological record (Noffke et al., 2006; Heubeck, 2009; Gamper et al., 2012; Homann et al., 2015). These mats draped and stabilized horizontally laminated and rippled sandstones, and show an enrichment in fine-grained quartz and feldspar, as well as heavy mineral grains (zircon and rutile or anatase), likely caused by microbial baffling and trapping, which is a commonly observed in epibenthic microbial mats (Gerdes et al., 2000). Microbial-mat-associated structures such as eroded mat fragments (mat chips), macroscopic tufts, shrinkage cracks, silicified gas domes and lenses, and subvertical fluid-escape structures are indicative for a former cohesive consistency and very common features in these deposits supporting the biogenic origin of the mats (Fig. 12B-D; Heubeck, 2009; Homann et al., 2015, 2016, 2018), while microbial wrinkle structures previously reported by Noffke et al. (2006) have not been observed in any of the follow-up studies. A detailed study

of the sedimentological and paleoenvironmental context of these fossil mats revealed that they are laterally traceable for ~15 km in a ~1000 m-thick succession in the lower part of the Saddleback Syncline and show distinct morphological adaptations to different hydrodynamic settings: (1) planar-type in coastal floodplain, (2) wavy-type in intertidal, and (3) tufted-type in upper inter- to supratidal facies (Homann et al., 2015). Such facies dependent changes in the prevalent mat morphotypes are to be expected in a dynamic, tidally-influenced coastal environment and serve as an additional biogenicity indicator (Allwood et al., 2006; Brasier et al., 2006). Moreover, the widespread occurrence of these fossil mats is consistent with a primary, microbially mediated, cohesive erosion-resistant relief on the paleosurface that was locally deformed by migrating gases and fluids, and in places eroded and incorporated in mat-chip conglomerates.

Based on the restriction of the mats to shallow-water, photic zone environments and their apparent absence in subtidal settings, it is very likely that they were formed by phototrophic microbial communities (Noffke et al., 2006; Heubeck, 2009; Homann et al., 2015). In fact, the Moodies microbial mats show some striking morphological similarities to modern cyanobacterial mats e.g. from Bahar Alouane, Tunisia (Fig. 12A-D; Gerdes et al., 2000; Gerdes, 2007), Shark Bay, Australia (Jahnert and Collins, 2013), Texas Gulf Coast, USA (Bose and Chafetz, 2009), and the Red Sea of Saudi Arabia (Taj et al., 2014). Especially the occurrence of mats with macroscopic, 0.3-to-1 cm-high tufts that closely resemble tufted mats build by filamentous cyanobacteria (Fig. 12C), led to the conclusion that the tufted mats of the Moodies Group were perhaps build by ancestral cyanobacteria (Homann et al., 2015). Even tough, no geochemical data supporting the local presence of free oxygen (and thus oxygenic photosynthesis) at 3.22 Ga have been found so far in the Moodies Group, fossil evidence indicative for ancient gas production, accumulation, and migration is plentiful in the near vicinity of the mats. Now chert-filled cavities in the interior of some tufts likely represent silicified gas bubbles that were trapped within the mat fabric, which is a common feature in cyanobacterial mats that produce oxygen-rich bubbles with strikingly similar morphologies (Fig. 12C; Bosak et al., 2010; Homann et al., 2015). Other types of silicified cavities include domes and bedding parallel lenses beneath the fossil mats that either formed through accumulation of gases produced by metabolic activity, due to the decay of organic matter, or alternatively by tidal-driven hydraulic pumping of the ambient air trapped in pore space (Figs. 12D and 14; Homann et al., 2016). Some of these cavities where also inhabited by microbial communities (see below in 5.2).

Besides the main mat occurrence in the tidal marine deposits of the Saddleback Syncline, fossil microbial mats also have been identified in the Dycedale Syncline (Homann et al., 2018), where a large variety of sedimentary structures indicates that this succession records a transition from alluvial-fluvial (terrestrial) to tide-influenced marine sedimentation (Heubeck and Lowe, 1994; Eriksson et al., 2006; Heubeck et al., 2016). These terrestrial mats occur confined to fluvial deposits at the base of a transgressive sequence that gradually deepens upward through deltaic, and medium-energy tidal, into subtidal siliciclastic deposits.

They are interbedded with gravely sandstones, drape conglomerate beds, are plastically deformed by 10- to 50-cm-high fluid-escape structures, and commonly experienced periods of subaerial exposure and desiccation evidenced by associated desiccation cracks (Fig. 13A and B). The terrestrial microbial mats of the Dycedale Syncline currently represent the oldest direct fossil trace for life on land (Homann et al., 2018). Overgrowth rims in pyrites from Moodies Group paleosols show signs of biogenic sulfur fractionation ( $\delta^{34}\text{S}_{\text{VCDT}}$  values between  $-20\text{‰}$  and  $-24.5\text{‰}$ ) and provide additional geochemical evidence for the presence of a Paleoarchean terrestrial biosphere (Nabhan et al., 2016a, b). Compared to the marine mats the carbonaceous laminae of terrestrial mats are similarly well preserved, but with up to 4 mm of preserved thickness often thicker than their marine counterparts (Fig. 11A and B; Fig. 13C). They are composed of a dense meshwork of interwoven filament-like microstructures that envelop fine-grained detrital particles whose long axes are preferentially aligned parallel to bedding (Fig. 13D and E; Homann et al., 2018). Individual carbonaceous filamentous structures are 1–3  $\mu\text{m}$  in diameter and resemble modern biofilm-forming, filamentous microorganisms. In places, a notable enrichment of tourmaline minerals can be observed in the mat fabric, which has also been reported from the stromatolitic laminae of the Mendon Formation (Byerly et al., 1986; Byerly and Palmer, 1991) and might be driven by evaporitic processes, but certainly demands further investigations. Raman spectroscopic analyses confirmed that both the terrestrial and marine mats are composed of organic carbon that has experienced similar peak temperatures of  $\sim 365^\circ\text{C}$ , consistent with the metamorphic grade of the Moodies Group (Xie et al., 1997; Tice et al., 2004) and thus demonstrating their synsedimentary origin and biogenicity (Homann et al., 2018). A detailed study of Homann et al. (2018) documented a significant difference in the biogeochemical cycling of carbon and nitrogen in terrestrial and marine mats. The preserved organic matter in the terrestrial mats shows  $\delta^{13}\text{C}_{\text{org}}$  values ranging between  $-23.6\text{‰}$  and  $-17.9\text{‰}$  (mean =  $-21.2\text{‰}$ ;  $n = 36$ ) and  $\delta^{15}\text{N}$  values between  $+1.9\text{‰}$  and  $+5.6\text{‰}$  (mean =  $+4.3\text{‰}$ ;  $n = 10$ ), in contrast to marine mats that show  $\delta^{13}\text{C}_{\text{org}}$  values ranging between  $-33.9\text{‰}$  and  $-21.3\text{‰}$  (mean =  $-27.4\text{‰}$ ;  $n = 30$ ) and  $\delta^{15}\text{N}$  values between  $-0.7\text{‰}$  and  $+3.1\text{‰}$  (mean =  $+1.8\text{‰}$ ;  $n = 10$ ). This  $\delta^{13}\text{C}_{\text{org}}$  composition of the terrestrial mats is consistent with autotrophic carbon fixation through the Calvin–Benson cycle, while  $\delta^{13}\text{C}_{\text{org}}$  values of the marine mats are best explained by carbon fixation via the Wood–Ljungdahl pathway, which includes acetogenic bacteria, methanogens and sulfate reducers. The observed trend in the Moodies Group microbial mats with  $\delta^{15}\text{N}$  values from as low as  $-1\text{‰}$  (marine) to up to  $+5\text{‰}$  (terrestrial) likely reflects increasing fixed-nitrogen (i.e., nitrate, nitrite or ammonium) and conversion to  $\text{N}_2\text{O}/\text{N}_2$  in the terrestrial habitats, which further suggests that they possessed a fundamentally different respiratory community at depth in the mat, one that must have been sufficiently oxygenated for aerobic Nitrogen cycling (Ader et al., 2016; Stüeken et al., 2016). Alternatively, the contrasting nitrogen isotope compositions between terrestrial and marine settings could be related to a

constant flux of atmospherically-fixed nitrogen on the early land surface that was probably too diffuse to be a significant source of fixed nitrogen to the marine biosphere (Homann et al., 2018).

## 5.2 Cavity-dwelling life

Lens-shaped, laterally tapering cavities, up to tens of centimeters in width and <0.5 cm in height, frequently occur beneath fossil microbial mat in intertidal deposits of the Saddleback Syncline (Fig. 14A; Homann et al., 2016). The silicified cavities resemble gas-filled, fenestral hollows in modern coastal environments that commonly form beneath cohesive, impermeable microbial mats and mat-bound sediments (Gerdes et al., 2000; Schieber et al., 2007). Due to the presence of carbonaceous laminations and wisps these chert lenses were initially interpreted as partially silicified epibenthic microstromatolites or thick mucilaginous mats (Heubeck 2009; Gamper et al., 2011), however, Homann et al. (2016) reported the additional presence of pendant columnar microstromatolites attached to the ceilings of former cavities and concluded that they must have accreted downwards in an open void space of synsedimentary origin (Fig. 14B-E). This gravity-oriented geometry and the downward-accretionary growth habit is well known from cavity-dwelling microorganisms (coelobionts; Kobluk and James, 1979; Jakubowicz et al., 2014), which have also been reported from synsedimentary cavities beneath microbial mats in sandstones of the Neoarchean Fortescue Group in Australia (Rasmussen et al., 2009). In places, sub-circular to ovoid-shaped fenestrae (~500 µm in diameter) that resemble trapped gas bubbles occur wedged between the carbonaceous laminae (Fig. 14C). SEM observations of the cavity-filling cherts reveal the presence of: (1) polygonal structures after HF etching for 28 days, interpreted as remnants of extracellular polymeric substance (EPS, Gamper et al., 2012), and (2) a meshwork of interwoven filamentous molds of likely biogenic origin that is completely embedded in the chert (Fig. 14F; unetched samples, Homann et al., 2016). The non-branching filaments (0.3–0.5 µm in diameter, n = 180) display a subdivision in regularly spaced, ~2-µm- long, rod-shaped segments and have a tubular morphology in cross section (Fig. 14G and H). Bulk carbon isotope measurements of the chert-bearing sandstones show  $\delta^{13}\text{C}_{\text{org}}$  values between -23.8‰ and -14.1‰ (mean = -20.5‰, n = 15; Gamper et al., 2012), however, *in situ* measurements of the carbonaceous laminae within the chert-cemented cavities yield  $\delta^{13}\text{C}_{\text{org}}$  values ranging between -32.3‰ and -21.3‰ (mean = -26.5‰; n = 12) that are probably more representative. These values are consistent with a purely chemotrophic or a photosynthetic community of coelobionts and support the biogenicity of the oldest evidence for cavity-dwelling life on Earth (Homann et al., 2016). Moreover, these findings support the view the cavities were among the first ecological niches to have been occupied by early microbial communities.

## 5.3 Organic-walled microfossils

Carbonaceous spheroidal microstructures, 31–300  $\mu\text{m}$  in diameter (mean=122  $\mu\text{m}$ ,  $n=98$ ), have been identified in bedded siltstones and shales from underground drill cores that were assigned to the Clutha Formation and drilled 600m below the surface in the Agnes gold mine, Moodies Hills Block (Javaux et al., 2010). The carbonaceous structures are visible in petrographic thin sections and resistant to extraction via acid maceration (Fig. 15A-D). They show wrinkled and folded textures, a ~160-nm-thick wall with a homogenous ultrastructure and were interpreted as flattened, hollow, and partially degraded, organic-walled vesicles with preserved cell lumen (Fig. 15E-F; Javaux et al., 2010). Bulk carbon isotopes measurements show a large spread in  $\delta^{13}\text{C}_{\text{org}}$  values ranging between -16.4% and -28.3%, with an average of -22.4% ( $n=22$ ), but no difference in the  $\delta^{13}\text{C}_{\text{org}}$  values between samples with and without microfossils has been observed. Consequently, such bulk measurements might not be very useful in constraining the biogenicity of the microstructures, however their carbonaceous composition and syngenetic origin is supported by Raman microspectroscopy. Based on their taphonomy and for the Paleoproterozoic uncommonly large size, Javaux et al. (2010) and Buick (2010). Javaux et al. (2010) concluded that the organic-walled microfossils might either represent remnants of extinct prokaryotes, colonial envelopes of cyanobacteria, or even eukaryotes. To unravel the biological affinity of these acritarchs remains the task for future investigations, which should ideally also aim to identify the microstructures in outcrop samples in order to further constrain their habitat and explore their possible relationship with the widespread, shallow-water microbial mats of the Moodies Group.

## 6. Discussion

### 6.1 Evidence of Paleoproterozoic life in the BGB and comparison to the PGBs

Traces of ancient life in the BGB occur mainly confined to bedded, carbonaceous cherts of the Onverwacht Group and the siliciclastic deposits of the Moodies Group. Preserved biosignatures in these deposits include putative microfossils of filamentous, spheroidal, and lenticular shape, stromatolites, and microbial mats. Filamentous microfossils occur very rarely in cherts of the Onverwacht Group but their biogenicity remains equivocal (Walsh and Lowe, 1985; Walsh 1992, 2010). The rod-shaped filamentous molds preserved in early silicified, syndepositional cavities of the Moodies Group resemble in shape and size microbial filaments and also their depositional context, beneath intertidal microbial mats, supports a biogenic origin (Homann et al., 2016). Spheroidal microstructures with carbonaceous walls, resembling coccoidal cells, belong to the most common group of putative microfossils in the Onverwacht Group but the assessment of their biogenicity is in most cases extremely challenging due to their simple, often symmetrical morphology that can be easily generated abiogenetically in form of e.g. fluid inclusions, vesicles, and spheroidal crystallites (Schopf and Walther 1983; Brasier et al., 2006). Solely, the spheroidal, cell-like objects reported

by Glikson et al. (2008) from the Hooggenoeg Formation and the large, organic-walled spheroids described by Javaux et al. (2010) from the Moodies Group have a well-established biogenicity. However, the biological affinity of the latter and the reason for their unusually large size currently remains unknown. Lenticular structures preserved in the Buck Reef Chert (Walsh 1992; Oehler et al., 2017) and probably also other cherts of the upper Onverwacht Group (Pflug 1966, 1967; Pflug et al., 1969) belong to the earliest reported and currently best studied microfossils in the BGB. Remains of these, likely planktonic, microorganisms have also been reported from the 3.45 Ga Strelley Pool Formation and the ~3 Ga Farrel Quartzite in the Pilbara Craton where their biogenicity is reasonably well established (e.g. Oehler et al., 2009, 2017; Sugitani et al. 2007, 2010, 2013; House et al., 2013; Kozawa et al., 2018). The morphologically similar specimens from Australia occur in the same depositional context and show strikingly similar mean  $\delta^{13}\text{C}_{\text{org}}$  values ( $-37.0\%$  and  $-36.1\%$ ) in comparison to their South African counterparts with a mean  $\delta^{13}\text{C}_{\text{org}}$  value of  $-37.3\%$  (Oehler et al., 2017). Abiogenic models for the formation of similar-looking structures derived from reworked vesicular volcanic glass exists (Wacey et al., 2018a, 2018b), however these pseudo-fossils do not resemble the same morphological and microstructural complexity (Alleon et al., 2018; Kozawa et al., 2018). Nevertheless, the occurrence of such pseudo-fossil examples highlights again the paramount importance of detailed micro- and nanoscale analysis in the evaluation of the biogenicity of putative microfossils. Additionally, future studies of microfossil-bearing cherts of the Onverwacht Group should always be accompanied by detailed analysis of the stratigraphic context and depositional facies, in combination with *in situ* geochemical analysis of the microfossils themselves and their encasing mineral matrix.

Stromatolites, generally considered as the most ancient macroscopically-visible traces for life on Earth, are surprisingly rare and currently not as well documented in the BGB in comparison to the PGBs, where the oldest unequivocal biogenic examples occur preserved in the 3.45 Ga Strelley Pool Formation (Allwood, et al 2006) and possibly also in the 3.48 Ga Dresser Formation (Fig. 16; Walter et al., 1980; Van Kranendonk et al., 2008). However, the often morphological very simple, laminated, domal to conical structures of Archean stromatolites can be easily confused with secondary abiogenic structures, especially in the absence of indicative microfossils. A recent study of Allwood et al. (2018), highlighting the importance of morphological analysis in combination with geochemistry at appropriate scales, serves as a cautionary tale and strongly questions the biogenicity of previously reported putative stromatolites from 3.7 Ga old metacarbonate rocks of Greenland (Nutman et al., 2016). Compared to the greenstone belts in the Pilbara region, the documented deposit of the BGB contain only minor evidence of early carbonate environments, which is probably related to the predominance of volcanic and clastic deposition in combination with high sedimentation rates that made the conditions for stromatolite formation less favorable.

The most widespread, pervasive, and probably also oldest trace of ancient life in the BGB are the remnants of shallow-water microbial mats and biofilms. Mat-like laminations occur in almost all black-and-white-banded, carbonaceous cherts of the Onverwacht Group (Walsh 1992), but only the examples reported from the 3.472 Ga Middle Marker (Hickman-Lewis, et al, 2018), the 3.416 Ga Buck Reef Chert (Walsh and Lowe, 1999; Tice and Lowe, 2004a, 2006a, b; Tice, 2009; Tice et al., 2011), and the 3.334 Ga Josefsdal Chert (Westall et al., 2011, 2006, 2011, 2015) are reasonably well studied to support their biogenic origin. Especially the mats and microfossils preserved in the up to 400-m-thick Buck Reef Chert represent a particularly widespread (~50 km along strike), well-preserved and -documented record of the Paleoproterozoic life. Besides the necessity to carefully reinvestigate more potentially microfossil- and mat-bearing carbonaceous cherts in the BGB it is also crucial to further support the already existing claims for early life from these units with more detailed geochemical analysis such as e.g. carbon, nitrogen, and sulphur isotope data. The microbial mats preserved in the tidal and fluvial sandstones and conglomerates of the 3.22 Ga Moodies Group are unique and currently not known from equivalent deposits from Australia (Fig. 16; Noffke et al., 2006; Heubeck, 2009; Gamper et al., 2012; Homann et al., 2015, 2018). The quality of preservation of the delicate carbonaceous mat laminae, distinct morphotypes, and mat-associated cavities in these coarse-grained and gravely siliciclastic deposits is truly exceptional and implies a rapid fossilization driven by early diagenetic silicification of the sediments (Heubeck 2009; Homann et al., 2015). The observed difference in the biogeochemical cycling of carbon and nitrogen in tidal marine and fluvial microbial mats from the Moodies Group (Homann et al., 2018) has demonstrated the potential of detailed geochemical analysis, which can give valuable insights in the different carbon fixation pathways and ultimately helps to constrain the metabolism(s) of the mat-building microbial communities and should consequently also be applied more extensively to the mats preserved in the Onverwacht Group.

## 6.2 Habitats and paleoecology

Evidence for Paleoproterozoic life in the BGB have been reported from a wide range of paleoenvironments including shallow marine (e.g. Byerly et al., 1986; Tice and Lowe, 2004a; Heubeck 2009; Homann et al., 2015), fluvial (Homann et al., 2018), hydrothermal (Glikson et al., 2008; Westall et al., 2015), and possibly planktonic settings (Walsh 1992; Oehler et al., 2017), as well as from cryptic cavities in the shallow subsurface of intertidal deposits (Homann et al., 2016). Due to the general restriction of microbial mats to shallow-water, photic zone paleoenvironments of the BGB, the common notion is that they were at least in part composed of photosynthetic microbial communities and already had a high level of UV radiation tolerance, while the microorganisms thriving in a hydrothermal context or in cavities were likely dominated by chemotrophic communities. Nearly all of these early microbial communities must have been severely affected by distant impacts of large asteroids (20 to 50 km in diameter), which occurred between 3.470 Ga



and 3.225 Ga and are recorded in the BGB deposits by eight known ejecta layers (Fig. 2; Lowe and Byerly, 1986, 2018; Lowe et al., 1989). Besides impact-generated tsunamis it has been proposed that some of these catastrophic events might have been large enough to cause partial boiling and sterilization of the oceans and possibly triggered mass extinctions of low-temperature microbes, including most photosynthetic microorganisms (Sleep et al., 1989; Lowe and Byerly, 2015). The question of how exactly early life managed to survive these events or if the global ecosystem got entirely destroyed and biogenesis was reset currently remains open.

The Moodies Group ecosystem was particularly diverse, advanced, and well-adapted and includes large spheroidal microfossils, Earth's earliest evidence of cavity-dwelling microbes (coelobionts), widespread intertidal tufted microbial mats, laterally traceable for 15 km in a ~1000 m-thick succession, as well as erosion-resistant fluvial microbial mats. The latter represent the oldest known direct fossil evidence for terrestrial life on the continental surface and are ~500 Ma older than ~2.7 Ga old fluvio-lacustrine stromatolites and coelobionts preserved in the Fortescue Group (Tumbiana and Hardey Formation, Australia; Buick, 1992; Awramik and Buchheim, 2009; Rasmussen et al., 2009; Coffey et al., 2013) and fluvial stromatolites documented in the Ventersdorp Supergroup (South Africa; Buck, 1980). Based on the apparent morphological similarities between the shallow-marine microbial mats of the Moodies Group and modern cyanobacterial mats such as e.g. macroscopic tufts, evidence for gas production and accumulation in bubbles and domes, and their widespread occurrence and presumably fast growth rate, it has been proposed that they were perhaps build by ancestral cyanobacteria (Homann et al., 2015). A recent molecular clock study by Cardona et al. (2018) supports this interpretation and suggest that a primordial photosystem capable of oxidizing water to oxygen could have formed before the most recent common ancestor of cyanobacteria. Additionally, also the unusually large size of the organic-walled microfossils reported by Javaux et al. (2010) indirectly suggests the requirement and the availability of oxygen at 3.22 Ga, although no unequivocal geochemical signs for the local presence of free oxygen have been found so far in the Moodies Group.

## 7. Conclusions

The deposits of the Barberton Greenstone Belt host a large variety of convincing macro- and microscopic, as well as geochemical evidence for early microbial life. It was predominantly thriving in shallow marine environments in the photic zone but started to spread out to colonize fluvial habitats in emerged continental surface environments and also occupied the first ecological niches, such as subsurface cavities. Traces of ancient life in the BGB occur scattered throughout the entire stratigraphy confined to carbonaceous cherts of the Onverwacht Group and siliciclastic deposits of the Moodies Group. However, their identification is sometimes solely based on morphological attributes and not always accompanied by detailed and systematic

geochemical analysis at appropriate scales, which should be improved in future investigations. Due to their wealth of remarkably preserved microbial mats and microfossils, consistent lateral exposure for several tens of kilometers and thick stratigraphy, especially the deposits of the 3.416 Ga Buck Reef Chert and the sandstones of the 3.22 Ga Moodies Group represent a unique window into a diverse Paleoarchean biosphere. Based on its universal and outstanding geological and paleobiological value the Barberton-Makhonjwa Mountains were inscribed in the UNESCO World Heritage Site register in 2018, which will ultimately help to protect these exceptional outcrops for future studies of Earth's early evolution.

## Acknowledgements

This work was greatly supported by LabexMER ANR-10-LABX-19 and Prestige COFUND-GA-2013-609102 to M.H. Amongst many others, the author would especially like to thank Maud Walsh, Gary Byerly, Don Lowe, Christoph Heubeck, Dorothy Oehler, Wlady Altermann, and Andrew Knoll for their helpful comments. I am also indebted to Stefan Lalonde and Claire Earlie for useful discussions and comments on an earlier version of the manuscript.

## References

- Ader, M., Thomazo, C., Sansjofre, P., Busigny, V., Papineau, D., Laffont, R., Cartigny, P., Halverson, G.P., 2016. Interpretation of the nitrogen isotopic composition of Precambrian sedimentary rocks: Assumptions and perspectives. *Chem. Geol.* 429, 93–110. <https://doi.org/10.1016/j.chemgeo.2016.02.010>
- Alleon, J., Bernard, S., Le Guillou, C., Beyssac, O., Sugitani, K., Robert, F., 2018. Chemical nature of the 3.4 Ga Strelley Pool microfossils. *Geochemical Perspect. Lett.* 37–42. <https://doi.org/10.7185/geochemlet.1817>
- Allwood, A.C., Rosing, M.T., Flannery, D.T., Hurowitz, J.A., Heirwegh, C.M., 2018. Reassessing evidence of life in 3,700-million-year-old rocks of Greenland. *Nature*. <https://doi.org/10.1038/s41586-018-0610-4>
- Allwood, A.C., Walter, M.R., Kamber, B.S., Marshall, C.P., Burch, I.W., 2006. Stromatolite reef from the Early Archaean era of Australia. *Nature* 441, 714–718. <https://doi.org/10.1038/nature04764>
- Altermann, W., 2001. The oldest fossils of Africa – a brief reappraisal of reports from the Archean. *J.*

- African Earth Sci. 33, 427–436. [https://doi.org/10.1016/S0899-5362\(01\)00089-6](https://doi.org/10.1016/S0899-5362(01)00089-6)
- Anhaeusser, C.R., 1976. The geology of the sheba hills area of the Barberton Mountain Land, South Africa with particular reference to the Eureka Syncline. *Trans. Geol. Soc. S. Africa* 79, 253–280.
- Armstrong, R.A., Compston, W., de Wit, M., Williams, I.S., 1990. The stratigraphy of the 3.5–3.2 Ga Barberton Greenstone Belt revisited: a single zircon ion microprobe study. *Earth Planet. Sci. Lett.* 101, 90–106.
- Awramik, S.M., 1992. The oldest records of photosynthesis. *Photosynth. Res.* 33, 75–89. <https://doi.org/10.1007/BF00039172>
- Awramik, S.M., Buchheim, H.P., 2009. A giant, Late Archean lake system: The Meentheena Member (Tumbiana Formation; Fortescue Group), Western Australia. *Precambrian Res.* 174, 215–240. <https://doi.org/10.1016/j.precamres.2009.07.005>
- Banerjee, N.R., Simonetti, A., Banerjee, N.R., Sciences, E., Ontario, W., Na, O., 2007. Direct dating of Archean microbial ichnofossils Direct dating of Archean microbial ichnofossils. <https://doi.org/10.1130/G23534A.1>
- Barghoorn, E.S., 1971. The oldest fossils. *Sci. Am.* 224, 30–43.
- Barghoorn, E.S., Schopf, J.W., 1966. Microorganisms Three Billion Years Old from the Precambrian of South Africa. *Science* (80-. ). 152, 758–763. <https://doi.org/10.1126/science.152.3723.758>
- Bosak, T., Bush, J.W.M., Flynn, M.R., Liang, B., Ono, S., Petroff, a. P., Sim, M.S., 2010. Formation and stability of oxygen-rich bubbles that shape photosynthetic mats. *Geobiology* 8, 45–55. <https://doi.org/10.1111/j.1472-4669.2009.00227.x>
- Bose, S., Chafetz, H.S., 2009. Topographic control on distribution of modern microbially induced sedimentary structures (MISS): A case study from Texas coast. *Sediment. Geol.* 213, 136–149. <https://doi.org/10.1016/j.sedgeo.2008.11.009>
- Brasier, M., McLoughlin, N., Green, O., Wacey, D., 2006. A fresh look at the fossil evidence for early Archaean cellular life. *Philos. Trans. R. Soc. Lond. B. Biol. Sci.* 361, 887–902. <https://doi.org/10.1098/rstb.2006.1835>
- Brooks, J., Muir, M.D., Shaw, G., 1973. Chemistry and Morphology of Precambrian Microorganisms. *Nature* 244, 215–217. <https://doi.org/10.1038/244215a0>
- Brooks, J., Shaw, G., 1971. Evidence for Life in the Oldest Known Sedimentary Rocks—the Onverwacht Series Chert, Swaziland System of Southern Africa. *Grana* 11, 1–8. <https://doi.org/10.1080/00173137109427403>
- Buck, S.G., 1980. Stromatolite and ooid deposits within the fluvial and lacustrine sediments of the Precambrian Ventersdorp Supergroup of South Africa. *Precambrian Res.* 12, 311–330. [https://doi.org/10.1016/0301-9268\(80\)90033-9](https://doi.org/10.1016/0301-9268(80)90033-9)

- Buick, R., 2010. Early life: Ancient acritarchs. *Nature* 463, 885–886. <https://doi.org/10.1038/463885a>
- Buick, R., 1992. The antiquity of oxygenic photosynthesis: evidence from stromatolites in sulphate-deficient Archaean lakes. *Science* (80-. ). 255, 74–77. <https://doi.org/10.1126/science.11536492>
- Byerly, G.R., 1999. Komatiites of the Mendon Formation: Late-stage ultramafic volcanism in the Barberton Greenstone Belt, in: Lowe, D.R., Byerly, G.R. (Eds.), *Geologic Evolution of the Barberton Greenstone Belt, South Africa*. Geological Society of America, p. 0. <https://doi.org/10.1130/0-8137-2329-9.189>
- Byerly, G.R., Lowe, D.R., Heubeck, C., 2019. Geologic Evolution of the Barberton Greenstone Belt—A Unique Record of Crustal Development, Surface Processes, and Early Life 3.55–3.20 Ga, in: *Earth's Oldest Rocks*. Elsevier, pp. 569–613. <https://doi.org/10.1016/B978-0-444-63901-1.00024-1>
- Byerly, G.R., Lowe, D.R., Walsh, M.M., 1986. Stromatolites from the 3,300–3,500-Myr Swaziland Supergroup, Barberton Mountain Land, South Africa. *Nature* 319, 489–491.
- Byerly, G.R., Palmer, M.R., 1991. Tourmaline mineralization in the Barberton greenstone belt, South Africa: early Archean metasomatism by evaporite-derived boron. *Contrib. to Mineral. Petrol.* 107, 387–402. <https://doi.org/10.1007/BF00325106>
- Cardona, T., Sánchez-Baracaldo, P., Rutherford, A.W., Larkum, A.W., 2018. Early Archean origin of Photosystem II. *Geobiology* 4, e00548. <https://doi.org/10.1111/gbi.12322>
- Coffey, J.M., Flannery, D.T., Walter, M.R., George, S.C., 2013. Sedimentology, stratigraphy and geochemistry of a stromatolite biofacies in the 2.72Ga Tumbiana Formation, Fortescue Group, Western Australia. *Precambrian Res.* 236, 282–296. <https://doi.org/10.1016/j.precamres.2013.07.021>
- De Ronde, C.E.J., De Wit, M.J., 1994. Tectonic history of the Barberton greenstone belt, South Africa: 490 million years of Archean crustal evolution. *Tectonics* 13, 983–1005. <https://doi.org/10.1029/94TC00353>
- De Ronde, C.E.J., Kamo, S.L., 2000. An Archaean arc-arc collisional event: A short-lived (ca 3 Myr) episode, Weltevreden area, Barberton greenstone belt, South Africa. *J. African Earth Sci.* 30, 219–248. [https://doi.org/10.1016/S0899-5362\(00\)00017-8](https://doi.org/10.1016/S0899-5362(00)00017-8)
- De Wit, M.J., Furnes, H., R., 2011. Geology and tectonostratigraphy of the Onverwacht Suite, Barberton Greenstone Belt. *Precambrian Res.* 186, 28–50.
- de Wit, M.J., Hart, R., Martin, A., Abbott, P., 1982. Archean abiogenic and probable biogenic structures associated with mineralized hydrothermal vent systems and regional metasomatism, with implications for greenstone belt studies. *Econ. Geol.* 77, 1783–1802. <https://doi.org/10.2113/gsecongeo.77.8.1783>
- Engel, A.E.J., Nagy, B., Nagy, L.A., Engel, C.G., Kremp, G.O.W., Drew, C.M., 1968. Alga-Like Forms

- in Onverwacht Series, South Africa: Oldest Recognized Lifelike Forms on Earth. *Science* (80-. ). 161, 1005–1008. <https://doi.org/10.1126/science.161.3845.1005>
- Eriksson, K.A., 1979. Marginal marine depositional processes from the Archaean Moodies Group, Barberton Mountain Land; South Africa: Evidence and significance. *Precambrian Res.* 8, 153–182.
- Eriksson, K.A., 1977. Tidal deposits from the Archaean Moodies Group, Barberton Mountain Land, South Africa. *Sediment. Geol.* 18, 257–281.
- Fliegel, D., Simonetti, A., Furnes, H., 2010. In-situ dating of the Earth ' s oldest trace fossil. <https://doi.org/10.1016/j.epsl.2010.09.008>
- Furnes, H., 2004. Early Life Recorded in Archean Pillow Lavas. *Science* (80-. ). 304, 578–581. <https://doi.org/10.1126/science.1095858>
- Furnes, H., Banerjee, N.R., Staudigel, H., Muehlenbachs, K., McLoughlin, N., Wit, M. De, Kranendonk, M. Van, 2007. Comparing petrographic signatures of bioalteration in recent to Mesoarchean pillow lavas : Tracing subsurface life in oceanic igneous rocks 158, 156–176. <https://doi.org/10.1016/j.precamres.2007.04.012>
- Gamper, A., Heubeck, C., Demske, D., Hoehse, M., 2012. Composition and Microfacies of Archean Microbial Mats (Moodies Group, ca. 3.22 Ga, South Africa), in: Noffke, N., Chafetz, H.S. (Eds.), *Microbial Mats in Siliclastic Depositional Systems Through Time*. SEPM (Society for Sedimentary Geology), Tulsa, pp. 65–74. <https://doi.org/10.2110/sepmsp.101.065>
- Gerdes, G., 2007. Structures Left by Modern Microbial Mats in Their Host Sediments, in: Schieber, J., Bose, P.K., Eriksson, P., Banerjee, S., Sarkar, S., Altermann, W., Catuneanu, O. (Eds.), *Atlas of Microbial Mat Features Preserved within the Siliciclastic Rock Record*. Elsevier, Amsterdam, pp. 5–38. [https://doi.org/10.1016/S1574-1966\(07\)02001-9](https://doi.org/10.1016/S1574-1966(07)02001-9)
- Gerdes, G., Klenke, T., Noffke, N., 2000. Microbial signatures in peritidal siliciclastic sediments: a catalogue. *Sedimentology* 47, 279–308.
- Glikson, M., Duck, L.J., Golding, S.D., Hofmann, A., Bolhar, R., Webb, R., Baiano, J.C.F., Sly, L.I., 2008. Microbial remains in some earliest Earth rocks: Comparison with a potential modern analogue. *Precambrian Res.* 164, 187–200. <https://doi.org/10.1016/j.precamres.2008.05.002>
- Grosch, E.G., McLoughlin, N., 2014. Reassessing the biogenicity of Earth's oldest trace fossil with implications for biosignatures in the search for early life. *Proc. Natl. Acad. Sci.* 111, 8380–8385. <https://doi.org/10.1073/pnas.1402565111>
- Hall, A.L., 1918. The geology of the Barberton gold mining district. *Geol. Surv. South Africa Mem.* 9, 347.
- Heinrichs, T.K., Reimer, T., 1977. Geology and tectonostratigraphy of the Onverwacht Suite, Barberton greenstone belt, South Africa. *Econ. Geol.* 72, 1426–1441.

- Heubeck, C., 2009. An early ecosystem of Archean tidal microbial mats (Moodies Group, South Africa, ca. 3.2 Ga). *Geology* 37, 931–934. <https://doi.org/10.1130/G30101A.1>
- Heubeck, C., Bläsing, S., Grund, M., Drabon, N., Homann, M., Nabhan, S., 2016. Geological constraints on Archean (3.22 Ga) coastal-zone processes from the Dycedale Syncline, Barberton Greenstone Belt. *South African J. Geol.* 119, 495–518. <https://doi.org/10.2113/gssajg.119.3.495>
- Heubeck, C., Engelhardt, J., Byerly, G.R., Zeh, A., Sell, B., Luber, T., Lowe, D.R., 2013. Timing of deposition and deformation of the Moodies Group (Barberton Greenstone Belt, South Africa): Very-high-resolution of Archaean surface processes. *Precambrian Res.* 231, 236–262. <https://doi.org/10.1016/j.precamres.2013.03.021>
- Heubeck, C., Lowe, D.R., 1999. Sedimentary petrography and provenance of the Archean Moodies Group, Barberton Greenstone Belt, in: Lowe, D.R., Byerly, G.R. (Eds.), *Geologic Evolution of the Barberton Greenstone Belt, South Africa*. Geological Society of America Special Paper 329, pp. 259–286.
- Heubeck, C., Lowe, D.R., 1994a. Depositional and tectonic setting of the Archean Moodies Group, Barberton greenstone belt, South Africa. *Precambrian Res.* 68, 257–290.
- Heubeck, C., Lowe, D.R., 1994b. Late syndepositional deformation and detachment tectonics in the Barberton Greenstone Belt, South Africa. *Tectonics* 13, 1514–1536.
- Hickman-Lewis, K., Cavalazzi, B., Foucher, F., Westall, F., 2018. Most ancient evidence for life in the Barberton greenstone belt: Microbial mats and biofabrics of the ~3.47 Ga Middle Marker horizon. *Precambrian Res.* 312, 45–67. <https://doi.org/10.1016/j.precamres.2018.04.007>
- Hickman-Lewis, K., Westall, F., Cavalazzi, B., 2019. Traces of Early Life From the Barberton Greenstone Belt, South Africa, in: *Earth's Oldest Rocks*. Elsevier B.V., pp. 1029–1058. <https://doi.org/10.1016/B978-0-444-63901-1.00042-3>
- Hofmann, A., 2005. The geochemistry of sedimentary rocks from the Fig Tree Group, Barberton greenstone belt: Implications for tectonic, hydrothermal and surface processes during mid-Archaean times. *Precambrian Res.* 143, 23–49. <https://doi.org/10.1016/j.precamres.2005.09.005>
- Hofmann, A., Bolhar, R., 2007. Carbonaceous cherts in the Barberton greenstone belt and their significance for the study of early life in the Archean record. *Astrobiology* 7, 355–388. <https://doi.org/10.1089/ast.2005.0288>
- Hofmann, A., Harris, C., 2008. Silica alteration zones in the Barberton greenstone belt : A window into subsea floor processes 3.5 – 3.3 Ga ago. *Chem. Geol.* 257, 221–239. <https://doi.org/10.1016/j.chemgeo.2008.09.015>
- Homann, M., Heubeck, C., Airo, A., Tice, M.M., 2015. Morphological adaptations of 3.22 Ga-old tufted microbial mats to Archean coastal habitats (Moodies Group, Barberton Greenstone Belt, South

- Africa). *Precambrian Res.* 266, 47–64. <https://doi.org/10.1016/j.precamres.2015.04.018>
- Homann, M., Heubeck, C., Bontognali, T.R.R., Bouvier, A.S., Baumgartner, L.P., Airo, A., 2016. Evidence for cavity-dwelling microbial life in 3.22 Ga tidal deposits. *Geology* 44, 51–54. <https://doi.org/10.1130/G37272.1>
- Homann, M., Sansjofre, P., Van Zuilen, M., Heubeck, C., Gong, J., Killingsworth, B., Foster, I.S., Airo, A., Van Kranendonk, M.J., Ader, M., Lalonde, S. V, 2018. Microbial life and biogeochemical cycling on land 3,220 million years ago. *Nat. Geosci.* 11, 665–671. <https://doi.org/10.1038/s41561-018-0190-9>
- House, C.H., Oehler, D.Z., Sugitani, K., Mimura, K., 2013. Carbon isotopic analyses of ca. 3.0 Ga microstructures imply planktonic autotrophs inhabited earth's early oceans. *Geology* 41, 651–654. <https://doi.org/10.1130/G34055.1>
- Jahnert, R.J., Collins, L.B., 2013. Controls on microbial activity and tidal flat evolution in Shark Bay, Western Australia. *Sedimentology* 60, 1071–1099. <https://doi.org/10.1111/sed.12023>
- Jakubowicz, M., Berkowski, B., Belka, Z., 2014. Cryptic coral-crinoid “hanging gardens” from the Middle Devonian of southern Morocco. *Geology* 42, 119–122. <https://doi.org/10.1130/G35217.1>
- Javaux, E.J., Marshall, C.P., Bekker, A., 2010. Organic-walled microfossils in 3.2-billion-year-old shallow-marine siliciclastic deposits. *Nature* 463, 934–8. <https://doi.org/10.1038/nature08793>
- Karkhanis, S.N., 1977. Artifacts produced by chemical processing of samples for micropalaeontology and organic geochemistry - a note of caution. *Precambrian Res.* 4, 229–236. [https://doi.org/10.1016/0301-9268\(77\)90015-8](https://doi.org/10.1016/0301-9268(77)90015-8)
- Knauth, L.P., Lowe, D.R., 2003. High Archean climatic temperature inferred from oxygen isotope geochemistry of cherts in the 3.5 Ga Swaziland Supergroup, South Africa. *Bull. Geol. Soc. Am.* 115, 566–580. [https://doi.org/10.1130/0016-7606\(2003\)115<0566:HACTIF>2.0.CO;2](https://doi.org/10.1130/0016-7606(2003)115<0566:HACTIF>2.0.CO;2)
- Knoll, A.H., Barghoorn, E.S., 1977. Archean Microfossils Showing Cell Division from the Swaziland System of South Africa. *Science* (80-. ). 198, 396–398. <https://doi.org/10.1126/science.198.4315.396>
- Kobluk, D.R., James, N.P., 1979. Cavity-dwelling organisms in Lower Cambrian patch reefs from southern Labrador. *Lethaia* 12, 193–218. <https://doi.org/10.1111/j.1502-3931.1979.tb00997.x>
- Kozawa, T., Sugitani, K., Oehler, D.Z., House, C.H., Saito, I., Watanabe, T., Gotoh, T., 2018. Early Archean planktonic mode of life: Implications from fluid dynamics of lenticular microfossils. *Geobiology* 1–14. <https://doi.org/10.1111/gbi.12319>
- Kremer, B., Kaźmierczak, J., 2017. Cellularly preserved microbial fossils from ~3.4 Ga deposits of South Africa: A testimony of early appearance of oxygenic life? *Precambrian Res.* 295, 117–129. <https://doi.org/10.1016/j.precamres.2017.04.023>

- 885 Kröner, A., Byerly, G.R., Lowe, D.R., 1991. Chronology of early Archaean granite-greenstone evolution  
886 in the Barberton Mountain Land, South Africa, based on precise dating by single zircon  
887 evaporation. *Earth Planet. Sci. Lett.* 103, 41–54.
- 888 Kröner, A., Hegner, E., Wendt, J.I., Byerly, G.R., 1996. The oldest part of the Barberton granitoid-  
889 greenstone terrain, South Africa: evidence for crust formation between 3.5 and 3.7 Ga. *Precambrian*  
890 *Res.* 78, 105–124. [https://doi.org/10.1016/0301-9268\(95\)00072-0](https://doi.org/10.1016/0301-9268(95)00072-0)
- 891 Lamb, S., Paris, I., 1988. Post-onverwacht group stratigraphy in the SE part of the Archaean Barbeton  
892 greenstone belt. *J. African Earth Sci. (and Middle East)* 7, 285–306. [https://doi.org/10.1016/0899-](https://doi.org/10.1016/0899-5362(88)90074-7)  
893 [5362\(88\)90074-7](https://doi.org/10.1016/0899-5362(88)90074-7)
- 894 Lanier, W.P., Lowe, D.R., 1982. Sedimentology of the Middle Marker (3.4 Ga), Onverwacht Group,  
895 Transvaal, South Africa. *Precambrian Res.* 18, 237–260. [https://doi.org/10.1016/0301-](https://doi.org/10.1016/0301-9268(82)90012-2)  
896 [9268\(82\)90012-2](https://doi.org/10.1016/0301-9268(82)90012-2)
- 897 Lepot, K., Williford, K.H., Ushikubo, T., Sugitani, K., Mimura, K., Spicuzza, M.J., Valley, J.W., 2013.  
898 Texture-specific isotopic compositions in 3.4 Gyr old organic matter support selective preservation  
899 in cell-like structures. *Geochim. Cosmochim. Acta* 112, 66–86.  
900 <https://doi.org/10.1016/j.gca.2013.03.004>
- 901 Lowe, D.R., 1999a. Geologic evolution of the Barberton Greenstone Belt and vicinity, in: Lowe, D.R.,  
902 Byerly, G. (Ed.), *Special Paper 329: Geologic Evolution of the Barberton Greenstone Belt, South*  
903 *Africa. Geological Society of America*, pp. 287–312. <https://doi.org/10.1130/0-8137-2329-9.287>
- 904 Lowe, D.R., 1999b. Petrology and sedimentology of cherts and related silicified sedimentary rocks in the  
905 Swaziland Supergroup, in: Lowe, D.R., Byerly, G.R. (Eds.), *Geologic Evolution of the Barberton*  
906 *Greenstone Belt, South Africa. Geological Society of America*, p. 0. [https://doi.org/10.1130/0-8137-](https://doi.org/10.1130/0-8137-2329-9.83)  
907 [2329-9.83](https://doi.org/10.1130/0-8137-2329-9.83)
- 908 Lowe, D.R., 1999c. Shallow-water sedimentation of accretionary lapilli-bearing strata of the Msauli  
909 Chert: Evidence of explosive hydromagmatic komatiitic volcanism, in: *Special Paper 329: Geologic*  
910 *Evolution of the Barberton Greenstone Belt, South Africa. Geological Society of America*, pp. 213–  
911 232. <https://doi.org/10.1130/0-8137-2329-9.213>
- 912 Lowe, D.R., 1994. Accretionary history of the Archean Barberton greenstone belt (3.55–3.22 Ga),  
913 southern Africa. *Geology* 22, 1099–1102.
- 914 Lowe, D.R., Byerly, G.R., 2018. The terrestrial record of Late Heavy Bombardment. *New Astron. Rev.*  
915 81, 39–61. <https://doi.org/10.1016/j.newar.2018.03.002>
- 916 Lowe, D.R., Byerly, G.R., 2015. Geologic record of partial ocean evaporation triggered by giant asteroid  
917 impacts, 3.29–3.23 billion years ago. *Geology* 43, 535–538. <https://doi.org/10.1130/G36665.1>
- 918 Lowe, D.R., Byerly, G.R., 2007. Ironstone bodies of the Barberton greenstone belt, South Africa:



- Products of a Cenozoic hydrological system, not Archean hydrothermal vents! GSA Bull. 119, 65–87. <https://doi.org/10.1130/b25997.1>
- Lowe, D.R., Byerly, G.R., 1999. Stratigraphy of the west-central part of the Barberton Greenstone Belt, South Africa, in: Lowe, D.R., Byerly, G.R. (Eds.), *Geologic Evolution of the Barberton Greenstone Belt, South Africa*. Geological Society of America Special Paper 329, pp. 1–36.
- Lowe, D.R., Byerly, G.R., 1986. Early Archean silicate spherules of probable impact origin, South Africa and Western Australia. *Geology* 14, 83. [https://doi.org/10.1130/0091-7613\(1986\)14<83:EASSOP>2.0.CO;2](https://doi.org/10.1130/0091-7613(1986)14<83:EASSOP>2.0.CO;2)
- Lowe, D.R., Byerly, G.R., Asaro, F., Kyte, F.J., 1989. Geological and Geochemical Record of 3400-Million-Year-Old Terrestrial Meteorite Impacts. *Science* (80-. ). 245, 959–962. <https://doi.org/10.1126/science.245.4921.959>
- Lowe, D.R., Byerly, G.R., Heubeck, C., 2012. Geologic Map of the west-central Barberton Greenstone Belt, in: South Africa, Scale 1:25,000. Geological Society of America Map and Chart Series No. 103, Boulder. <https://doi.org/10.1130/2012.MCH103>
- Lowe, D.R., Knauth, L.P., 1977. Sedimentology of the Onverwacht Group (3.4 Billion Years), Transvaal, South Africa, and Its Bearing on the Characteristics and Evolution of the Early Earth. *J. Geol.* 85, 699–723. <https://doi.org/10.1086/628358>
- Lowe, D.R., Worrell, G.F., 1999. Sedimentology, mineralogy, and implications of silicified evaporites in the Kromberg Formation, Barberton Greenstone Belt, South Africa, in: *Special Paper 329: Geologic Evolution of the Barberton Greenstone Belt, South Africa*. Geological Society of America, pp. 167–188. <https://doi.org/10.1130/0-8137-2329-9.167>
- Mcloughlin, N., Grosch, E.G., Kilburn, M.R., Wacey, D., 2012. Sulfur isotope evidence for a Paleoproterozoic subseafloor biosphere, Barberton, South Africa 1031–1035. <https://doi.org/10.1130/G33313.1>
- Muir, M.D., Grant, P.R., 1976. Micropalaeontological evidence from the Onverwacht Group, South Africa, in: Windley, B. (Ed.), *The Early History of the Earth*. John Wiley & Sons, New York, pp. 595–608.
- Muir, M.D., Hall, D.O., 1974. Diverse microfossils in Precambrian Onverwacht group rocks of South Africa. *Nature* 252, 376–378. <https://doi.org/10.1038/252376a0>
- Nabhan, S., Lubert, T., Scheffler, F., Heubeck, C., 2016a. Climatic and geochemical implications of Archean pedogenic gypsum in the Moodies Group (~3.2 Ga), Barberton Greenstone Belt, South Africa. *Precambrian Res.* 275, 119–134. <https://doi.org/10.1016/j.precamres.2016.01.011>
- Nabhan, S., Wiedenbeck, M., Milke, R., Heubeck, C., 2016b. Biogenic overgrowth on detrital pyrite in ca. 3.2 Ga Archean paleosols. *Geology* 44, 763–766. <https://doi.org/10.1130/G38090.1>

- Nagy, B., Nagy, L.A., 1969. Early Pre-Cambrian Onverwacht Microstructures : Possibly the Oldest Fossils on Earth? *Nature* 223, 1226–1229. <https://doi.org/10.1038/2231226a0>
- Noffke, N., Eriksson, K.A., Hazen, R.M., Simpson, E.L., 2006. A new window into Early Archean life: Microbial mats in Earth's oldest siliciclastic tidal deposits (3.2 Ga Moodies Group, South Africa). *Geology* 34, 253. <https://doi.org/10.1130/G22246.1>
- Nutman, A.P., Bennett, V.C., Friend, C.R.L., Van Kranendonk, M.J., Chivas, A.R., 2016. Rapid emergence of life shown by discovery of 3,700-million-year-old microbial structures. *Nature* 537, 535–538. <https://doi.org/10.1038/nature19355>
- Oehler, D.Z., Schopf, J.W., Kvenvolden, K.A., 1972. Carbon Isotopic Studies of Organic Matter in Precambrian Rocks. *Science* (80-. ). 175, 1246–1248. <https://doi.org/10.1126/science.175.4027.1246>
- Oehler, D.Z., Walsh, M.M., Sugitani, K., Liu, M.C., House, C.H., 2017. Large and robust lenticular microorganisms on the young Earth. *Precambrian Res.* 296, 112–119. <https://doi.org/10.1016/j.precamres.2017.04.031>
- Oehler, D.Z., Walter, M.R., Sugitani, K., Allwood, A., Meibom, A., Mostefaoui, S., Selo, M., Thomen, A., Gibson, E.K., 2009. NanoSIMS : Insights to biogenicity and syngeneity of Archaean carbonaceous structures 173, 70–78. <https://doi.org/10.1016/j.precamres.2009.01.001>
- Otálora, F., Mazurier, A., Garcia-Ruiz, J.M., Van Kranendonk, M.J., Kotopoulou, E., El Albani, A., Garrido, C.J., 2018. A crystallographic study of crystalline casts and pseudomorphs from the 3.5 Ga dresser formation, Pilbara Craton (Australia). *J. Appl. Crystallogr.* 51, 1050–1058. <https://doi.org/10.1107/S1600576718007343>
- Pflug, H.D., 1967. Structured organic remains from the Fig Tree Series (Precambrian) of the Barberton mountain land (South Africa). *Rev. Palaeobot. Palynol.* 5, 9–29. [https://doi.org/10.1016/0034-6667\(67\)90205-9](https://doi.org/10.1016/0034-6667(67)90205-9)
- Pflug, H.D., 1966. Structured organic remains from the Fig Tree Series (Precambrian) of the Barberton Mountain land (South Africa). *Econ. Geol. Res. Unit, Univ. Witwatersrand, Johannesburg, Inform. Circ.* 28, 14.
- Pflug, H.D., Meinel, W., Neumann, K.H., Meinel, M., 1969. Entwicklungstendenzen des frühen Lebens auf der Erde. *Naturwissenschaften* 56, 10–14. <https://doi.org/10.1007/BF00599585>
- Rasmussen, B., Blake, T.S., Fletcher, I.R., Kilburn, M.R., 2009. Evidence for microbial life in synsedimentary cavities from 2.75 Ga terrestrial environments. *Geology* 37, 423–426. <https://doi.org/10.1130/G25300A.1>
- Schieber, J., Bose, P.K., Eriksson, P.G., 2007. Atlas of microbial mat features preserved within the siliciclastic rock record. Elsevier, Amsterdam.
- Schopf, J.W., 2004. Geochemical and submicron-scale morphologic analyses of individual Precambrian

- microorganisms. *Geochemical Soc. Spec. Publ.* 365–375.
- Schopf, J.W., 1975. Precambrian Paleobiology: Problems and Perspectives. *Annu. Rev. Earth Planet. Sci.* 3, 213–249. <https://doi.org/10.1146/annurev.ea.03.050175.001241>
- Schopf, J.W., Barghoorn, E.S., 1967. Alga-Like Fossils from the Early Precambrian of South Africa. *Science* (80-. ). 156, 508–512. <https://doi.org/10.1126/science.156.3774.508>
- Schopf, J.W., Walter, M.R., 1983. Archean microfossils: new evidence of ancient microbes, in: Schopf, J.W. (Ed.), *Earth's Earliest Biosphere: Its Origin and Evolution*. Princeton University Press, Princeton, pp. 214–239.
- Simpson, E.L., Eriksson, K.A., Mueller, W.U., 2012. 3.2 Ga eolian deposits from the Moodies Group, Barberton Greenstone Belt, South Africa: Implications for the origin of first-cycle quartz sandstones. *Precambrian Res.* 214–215, 185–191. <https://doi.org/10.1016/j.precamres.2012.01.019>
- Sleep, N.H., Zahnle, K.J., Kasting, J.F., Morowitz, H.J., 1989. Annihilation of ecosystems by large asteroid impacts on the early Earth. *Nature* 342, 139–142. <https://doi.org/10.1038/342139a0>
- Staudigel, H., Furnes, H., Dewit, M., 2015. Paleoarchean trace fossils in altered volcanic glass 112. <https://doi.org/10.1073/pnas.1421052112>
- Stüeken, E.E., Kipp, M.A., Koehler, M.C., Buick, R., 2016. The evolution of Earth's biogeochemical nitrogen cycle. *Earth-Science Rev.* 160, 220–239. <https://doi.org/10.1016/j.earscirev.2016.07.007>
- Sugitani, K., Grey, K., Allwood, A., Nagaoka, T., Mimura, K., Minami, M., Marshall, C.P., Van Kranendonk, M.J., Walter, M.R., 2007. Diverse microstructures from Archaean chert from the Mount Goldsworthy-Mount Grant area, Pilbara Craton, Western Australia: Microfossils, dubiofossils, or pseudofossils? *Precambrian Res.* 158, 228–262. <https://doi.org/10.1016/j.precamres.2007.03.006>
- Sugitani, K., Lepot, K., Nagaoka, T., Mimura, K., Van Kranendonk, M., Oehler, D.Z., Walter, M.R., 2010. Biogenicity of Morphologically Diverse Carbonaceous Microstructures from the *ca.* 3400 Ma Strelley Pool Formation, in the Pilbara Craton, Western Australia. *Astrobiology* 10, 899–920. <https://doi.org/10.1089/ast.2010.0513>
- Sugitani, K., Mimura, K., Nagaoka, T., Lepot, K., Takeuchi, M., 2013. Microfossil assemblage from the 3400Ma Strelley Pool Formation in the Pilbara Craton, Western Australia: Results form a new locality. *Precambrian Res.* 226, 59–74. <https://doi.org/10.1016/j.precamres.2012.11.005>
- Taj, R.J., Aref, M. a. M., Schreiber, B.C., 2014. The influence of microbial mats on the formation of sand volcanoes and mounds in the Red Sea coastal plain, south Jeddah, Saudi Arabia. *Sediment. Geol.* 311, 60–74. <https://doi.org/10.1016/j.sedgeo.2014.06.006>
- Tice, M.M., 2009. Environmental Controls on Photosynthetic Microbial Mat Distribution and Morphogenesis on a 3.42Ga Clastic-Starved Platform. *Astrobiology* 9, 989–1000.

- 1681  
1682  
1683 1021 Tice, M.M., Bostick, B.C., Lowe, D.R., 2004. Thermal history of the 3.5-3.2 Ga Onverwacht and Fig  
1684 1022 Tree Groups, Barberton greenstone belt, South Africa, inferred by Raman microspectroscopy of  
1685 1023 carbonaceous material. *Geology* 32, 37–40. <https://doi.org/10.1130/G19915.1>  
1687 1024 Tice, M.M., Lowe, D.R., 2006a. The origin of carbonaceous matter in pre-3.0 Ga greenstone terrains: A  
1688 1025 review and new evidence from the 3.42 Ga Buck Reef Chert. *Earth-Science Rev.* 76, 259–300.  
1690 1026 <https://doi.org/10.1016/j.earscirev.2006.03.003>  
1691 1027 Tice, M.M., Lowe, D.R., 2006b. Hydrogen-based carbon fixation in the earliest known photosynthetic  
1692 1028 organisms. *Geology* 34, 37. <https://doi.org/10.1130/G22012.1>  
1694 1029 Tice, M.M., Lowe, D.R., 2004. Photosynthetic microbial mats in the 3 , 416-Myr-old ocean. *Nature* 431,  
1695 1030 549–552. <https://doi.org/10.1038/nature02920.1>.  
1697 1031 Tice, M.M., Thornton, D.C.O., Pope, M.C., Olszewski, T.D., Gong, J., 2011. Archean Microbial Mat  
1698 1032 Communities. *Annu. Rev. Earth Planet. Sci.* 39, 297–319. [https://doi.org/10.1146/annurev-earth-](https://doi.org/10.1146/annurev-earth-040809-152356)  
1700 1033 [040809-152356](https://doi.org/10.1146/annurev-earth-040809-152356)  
1702 1034 Toulkeridis, T., Goldstein, S.L., Clauer, N., Kröner, A., Todt, W., Schidlowski, M., 1998. Sm-Nd, Rb-Sr  
1703 1035 and Pb-Pb dating of silicic carbonates from the early Archaean Barberton Greenstone Belt, South  
1704 1036 Africa: evidence for post-depositional isotopic resetting at low temperature. *Precambrian Res.* 92,  
1706 1037 129–144.  
1707 1038 Trower, E.J., Lowe, D.R., 2016. Sedimentology of the ~3.3Ga upper Mendon Formation, Barberton  
1709 1039 Greenstone Belt, South Africa. *Precambrian Res.* 281, 473–494.  
1710 1040 <https://doi.org/10.1016/j.precamres.2016.06.003>  
1712 1041 Van Kranendonk, M.J., Philippot, P., Lepot, K., Bodorkos, S., Pirajno, F., 2008. Geological setting of  
1713 1042 Earth's oldest fossils in the ca. 3.5 Ga Dresser Formation, Pilbara Craton, Western Australia.  
1714 1043 *Precambrian Res.* 167, 93–124. <https://doi.org/10.1016/j.precamres.2008.07.003>  
1716 1044 van Zuilen, M.A., Chaussidon, M., Rollion-Bard, C., Marty, B., 2007. Carbonaceous cherts of the  
1717 1045 Barberton Greenstone Belt, South Africa: Isotopic, chemical and structural characteristics of  
1719 1046 individual microstructures. *Geochim. Cosmochim. Acta* 71, 655–669.  
1720 1047 <https://doi.org/10.1016/j.gca.2006.09.029>  
1722 1048 Viljoen, M.J., Viljoen, R.P., 1969. An introduction to the geology of the Barberton granite-greenstone  
1723 1049 terrain. *Spec. Publ. Geol. Soc. S. Afr* 2, 9–28.  
1725 1050 Visser, D., 1956. The geology of the Barberton area. *Geol. Soc. S. Afr. Spec. Publ.* 15, 253.  
1726 1051 Wacey, D., 2012. Earliest evidence for life on Earth: An Australian perspective. *Aust. J. Earth Sci.* 59,  
1727 1052 153–166. <https://doi.org/10.1080/08120099.2011.592989>  
1729 1053 Wacey, D., 2009. Early Life on Earth. A Practical Guide, Topics in Geobiology , Vol. 31. Springer.  
1730 1054 Wacey, D., Fisk, M., Saunders, M., Eiloart, K., Kong, C., 2017. Critical testing of potential cellular  
1731  
1732  
1733  
1734  
1735  
1736

- structures within microtubes in 145 Ma volcanic glass from the Argo Abyssal Plain. *Chem. Geol.* 466, 575–587. <https://doi.org/10.1016/j.chemgeo.2017.07.006>
- Wacey, D., Noffke, N., Saunders, M., Guagliardo, P., Pyle, D.M., 2018a. Volcanogenic Pseudo-Fossils from the ~3.48 Ga Dresser Formation, Pilbara, Western Australia. *Astrobiology* 18, ast.2017.1734. <https://doi.org/10.1089/ast.2017.1734>
- Wacey, D., Saunders, M., Kong, C., 2018b. Remarkably preserved tephra from the 3430 Ma Strelley Pool Formation, Western Australia: Implications for the interpretation of Precambrian microfossils. *Earth Planet. Sci. Lett.* 487, 33–43. <https://doi.org/10.1016/j.epsl.2018.01.021>
- Walsh, M.M., 2004. Evaluation of Early Archean Volcaniclastic and Volcanic Flow Rocks as Possible Sites for Carbonaceous Fossil Microbes. *Astrobiology* 4, 429–437. <https://doi.org/10.1089/ast.2004.4.429>
- Walsh, M.M., 1992. Microfossils and possible microfossils from the Early Archean Onverwacht Group, Barberton Mountain Land, South Africa. *Precambrian Res.* 54, 271–293.
- Walsh, M.M., Lowe, D.R., 1999. Modes of accumulation of carbonaceous matter in the Early Archean: a petrographic and geochemical study of the carbonaceous cherts of the Swaziland Supergroup, in: Lowe, D.R., Byerly, G.R. (Eds.), *Geologic Evolution of the Barberton Greenstone Belt, South Africa*. Geological Society of America Special Paper 329, pp. 115–132.
- Walsh, M.M., Lowe, D.R., 1985. Filamentous microfossils from the 3,500-Myr-old Onverwacht Group, Barberton Mountain Land, South Africa. *Nature* 314, 530–531.
- Walter, M.R., Buick, R., Dunlop, J.S.R., 1980. Stromatolites 3,400–3,500 Myr old from the North Pole area, Western Australia. *Nature*. <https://doi.org/10.1038/284443a0>
- Westall, F., Campbell, K.A., Bréhéret, J.G., Foucher, F., Gautret, P., Hubert, A., Sorieul, S., Grassineau, N., Guido, D.M., 2015. Archean (3.33 Ga) microbe-sediment systems were diverse and flourished in a hydrothermal context. *Geology* 43, 615–618. <https://doi.org/10.1130/G36646.1>
- Westall, F., Cavalazzi, B., Lemelle, L., Marrocchi, Y., Rouzaud, J.N., Simionovici, A., Salomé, M., Mostefaoui, S., Andreazza, C., Foucher, F., Toporski, J., Jauss, A., Thiel, V., Southam, G., MacLean, L., Wirick, S., Hofmann, A., Meibom, A., Robert, F., Défarge, C., 2011. Implications of in situ calcification for photosynthesis in a ~3.3Ga-old microbial biofilm from the Barberton greenstone belt, South Africa. *Earth Planet. Sci. Lett.* 310, 468–479. <https://doi.org/10.1016/j.epsl.2011.08.029>
- Westall, F., de Ronde, C.E., Southam, G., Grassineau, N., Colas, M., Cockell, C., Lammer, H., 2006. Implications of a 3.472–3.333 Gyr-old subaerial microbial mat from the Barberton greenstone belt, South Africa for the UV environmental conditions on the early Earth. *Philos. Trans. R. Soc. B Biol. Sci.* 361, 1857–1876. <https://doi.org/10.1098/rstb.2006.1896>

- Westall, F., De Wit, M.J., Dann, J., Van der Gaast, S., De Ronde, C.E.J., Gerneke, D., 2001. Early  
archean fossil bacteria and biofilms in hydrothermally-influenced sediments from the Barberton  
greenstone belt, South Africa. *Precambrian Res.* 106, 93–116. [https://doi.org/10.1016/S0301-9268\(00\)00127-3](https://doi.org/10.1016/S0301-9268(00)00127-3)
- Westall, F., Hickman-Lewis, K., Hinman, N., Gautret, P., Campbell, K.A., Bréhéret, J.G., Foucher, F.,  
Hubert, A., Sorieul, S., Dass, A.V., Kee, T.P., Georgelin, T., Brack, A., 2018. A Hydrothermal-  
Sedimentary Context for the Origin of Life. *Astrobiology* 18, 259–293.  
<https://doi.org/10.1089/ast.2017.1680>
- Williford, K.H., Ushikubo, T., Lepot, K., Kitajima, K., Hallmann, C., Spicuzza, M.J., Kozdon, R.,  
Eigenbrode, J.L., Summons, R.E., Valley, J.W., 2016. Carbon and sulfur isotopic signatures of  
ancient life and environment at the microbial scale: Neoarchean shales and carbonates. *Geobiology*  
14, 105–128. <https://doi.org/10.1111/gbi.12163>
- Williford, K.H., Ushikubo, T., Schopf, J.W., Lepot, K., Kitajima, K., Valley, J.W., 2013. Preservation  
and detection of microstructural and taxonomic correlations in the carbon isotopic compositions of  
individual Precambrian microfossils. *Geochim. Cosmochim. Acta* 104, 165–182.  
<https://doi.org/10.1016/j.gca.2012.11.005>
- Xie, X., Byerly, G.R., Ferrell Jr., R.E., 1997. Ilb trioctahedral chlorite from the Barberton greenstone belt:  
crystal structure and rock composition constraints with implications to geothermometry. *Contrib. to  
Mineral. Petrol.* 126, 275–291. <https://doi.org/10.1007/s004100050250>

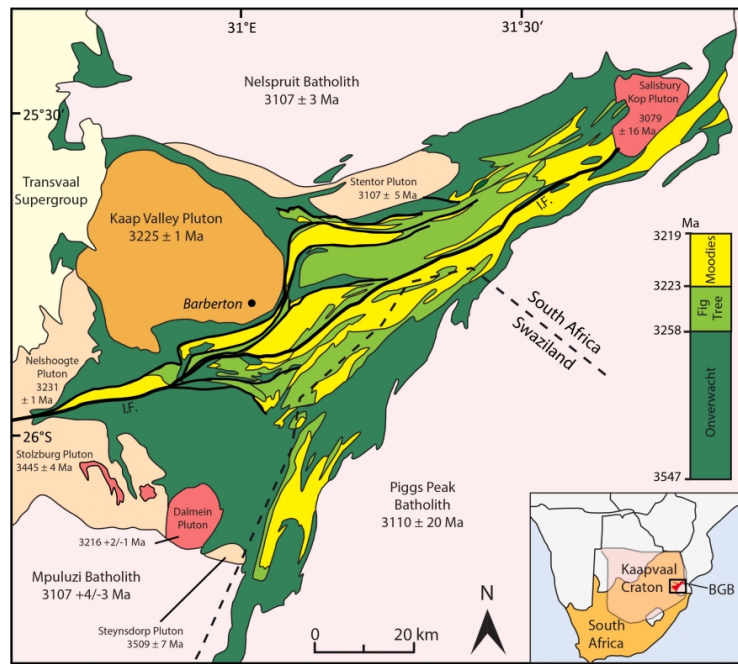


Fig. 1. Geological map of the Barberton Greenstone Belt (BGB) of South Africa and Swaziland and its surrounding plutons in the eastern part of the Kaapvaal Craton. The Barberton Supergroup comprises from base to top the Onverwacht, Fig Tree, and Moodies Group.





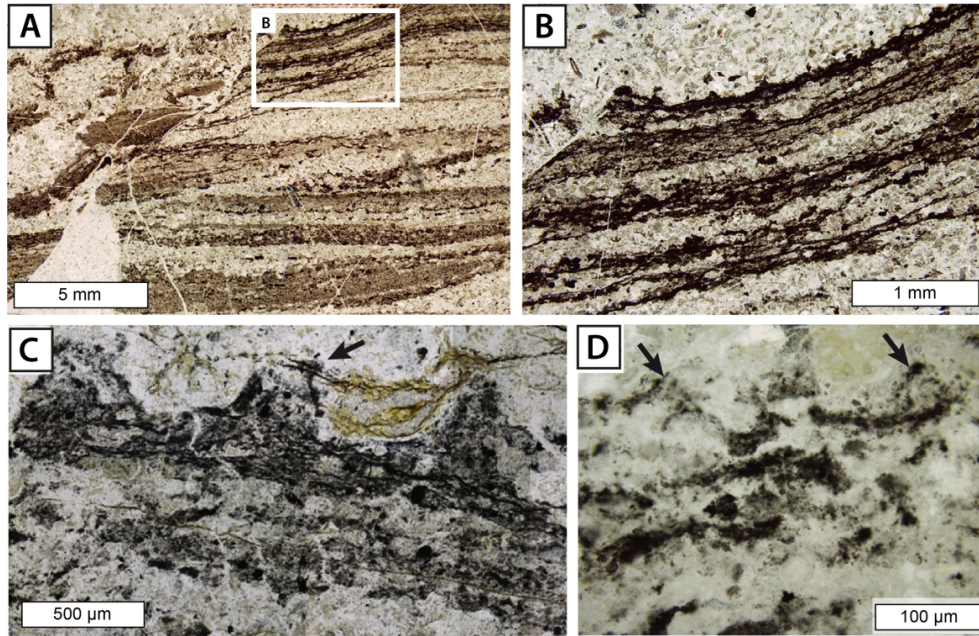


Fig. 3. Photomicrographs of carbonaceous laminations from silicified volcaniclastic sediments of the 3.47 Ga Middle Marker interpreted as remnants of microbial mats. A) Multi-layered mats on horizontally-laminated and cross-bedded sediments, disrupted by secondary fracture. B) Close-up view of crinkly, 'micro-tufted' laminations. C and D) Laminations with secondary 'pseudo-tufted' morphology (arrows), which likely formed due to plastic deformation. *Images (A-D) from Hickman-Lewis et al. (2018).*

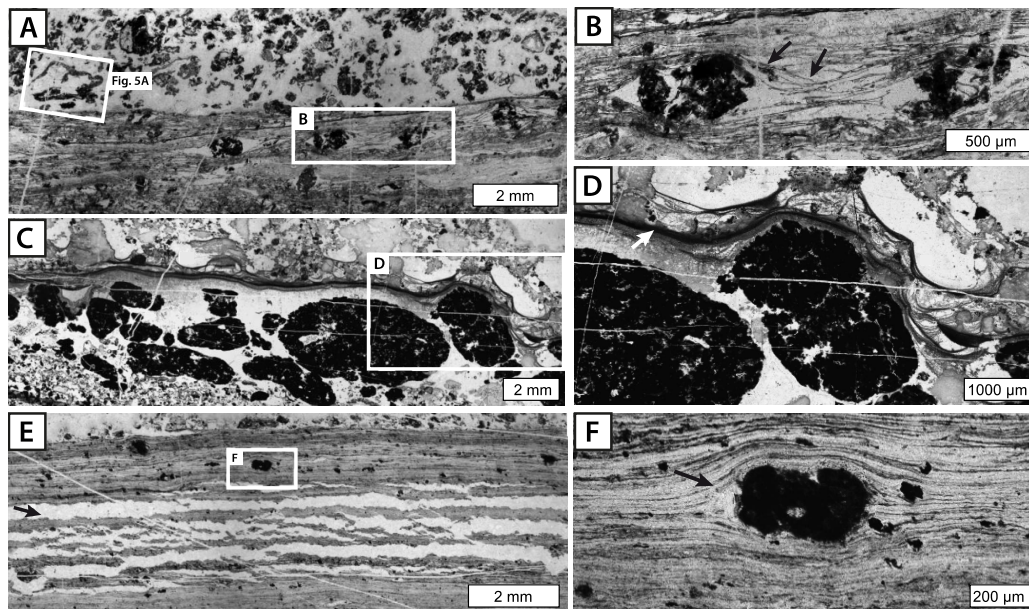


Fig. 4. Photomicrographs of morphologically diverse types of carbonaceous laminations preserved in the 3.42 Ga Buck Reef Chert and interpreted as fossil microbial mats. A and B) Alpha-type laminations loosely draping trapped grains (arrows) and overlain by detrital sediment layer with eroded mat fragment. C and D) Beta-type laminations with fine meshworks of filament-like strands that drape underlying detrital carbonaceous and silica grains (arrow). E) Gamma-type laminations dissected by early diagenetic silica veins subparallel to bedding (arrow), likely formed due to fluid escape from the sediment. F) Close-up view showing flat carbonaceous laminations, which tightly drape a detrital grain (arrow). *Images (A-F) from Tice (2009).*

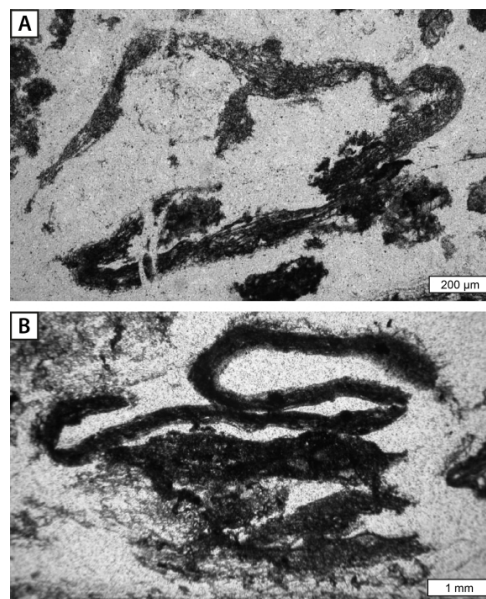


Fig. 5. Photomicrographs of eroded and rolled-up microbial mat fragments from the Buck Reef Chert. A) Close-up view of boxed area in Fig. 4A showing a plastically-deformed segment of alpha-type mat. B) Large, rolled-up fragment of a beta-type mat. *Image (A) from Tice (2009) and (B) from Tice and Lowe 2006b.*



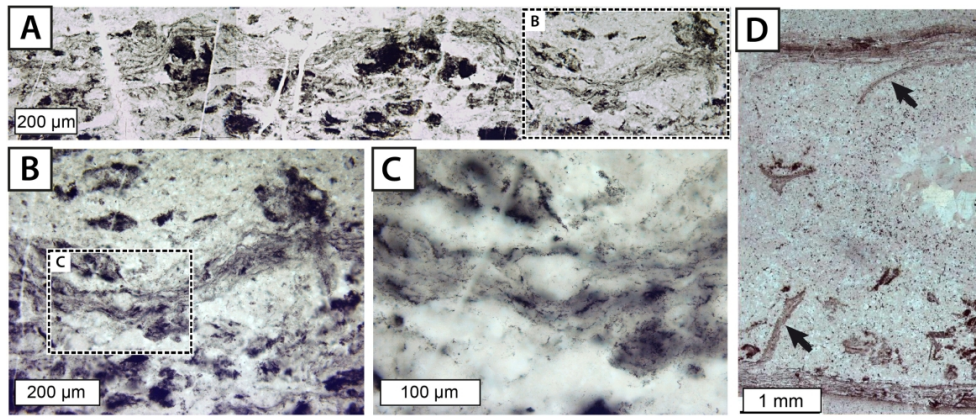


Fig. 6. Photomicrographs of microbial biofilms preserved in the 3.33 Ga Josefsdal Chert. A) Wispy anastomosing laminations that coat and stabilize the underlying sediments. B and C) Close-up views of the fine carbonaceous layers. D) Partially eroded fragments facing down and upwards (arrows) indicate pliable consistency of the biofilms. *Images (A-C) from Westall et al. (2011); Image (D) from Westall et al. (2015).*

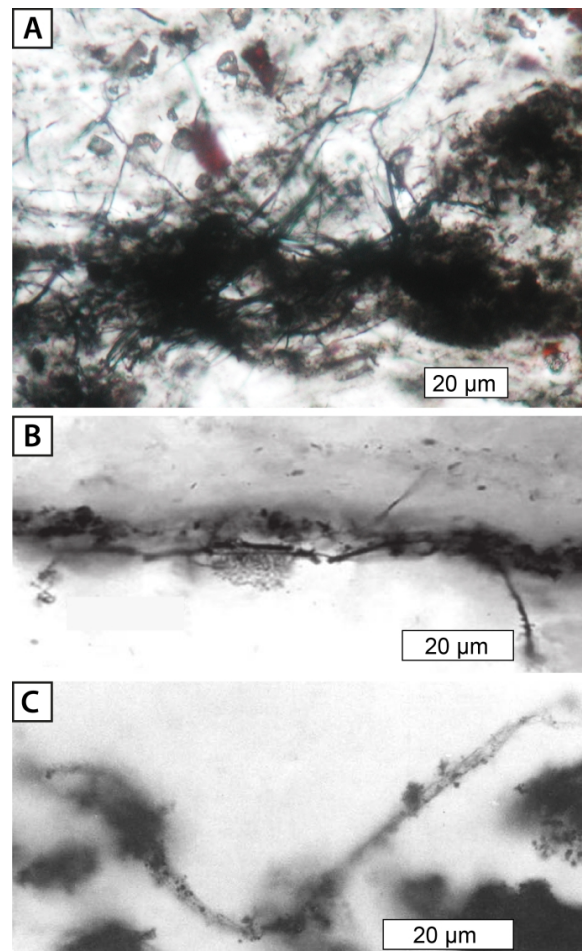


Fig. 7. Photomicrographs of filamentous microstructures from the Buck Reef Chert (Kromberg Formation). A) Interwoven clumps of filamentous microfossils. B) Hollow cylindrical filaments oriented subparallel to bedding. C) Solitary, slightly twisted hollow filament. *Image (A) courtesy of Maud M. Walsh; Image (B) from Walsh (2000); Image (C) from Walsh (1992).*

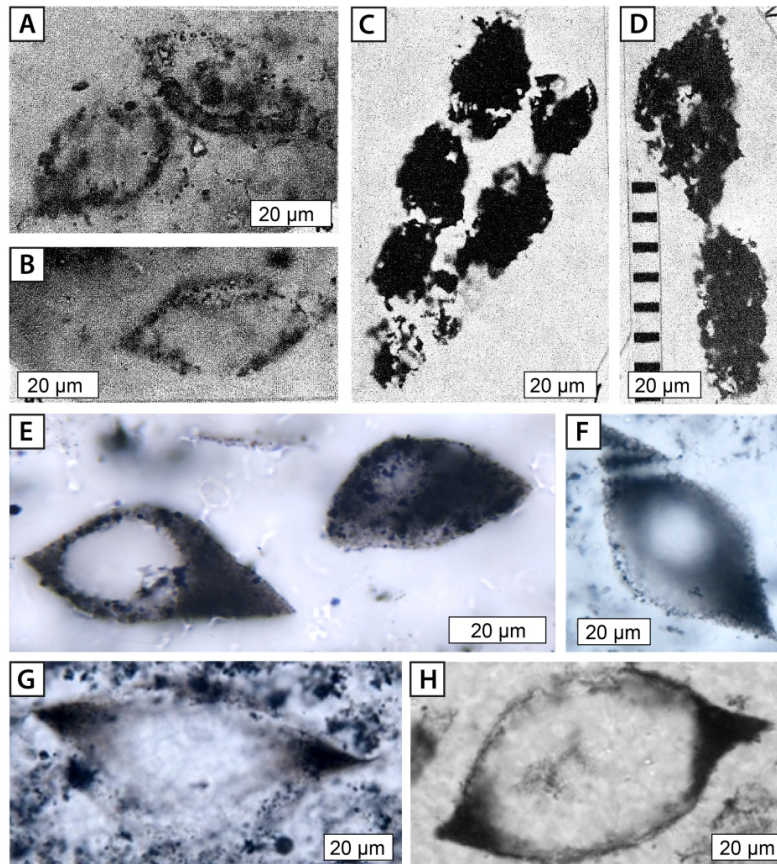


Fig. 8. Photomicrographs of lenticular structures interpreted as microfossils. A-D) Lenticular, disk-shaped objects with hollow centers and carbonaceous walls preserved in cherts from the Upper Onverwacht Group. Note that the structures occur isolated or in chain-like clusters of several specimen. (E-H) Morphologically very similar lenticular microfossils from the Buck Reef Chert. *Images (A-D) from Pflug (1966); Images (E-H) from Oehler et al. (2017), courtesy of Dorothy Z. Oehler.*

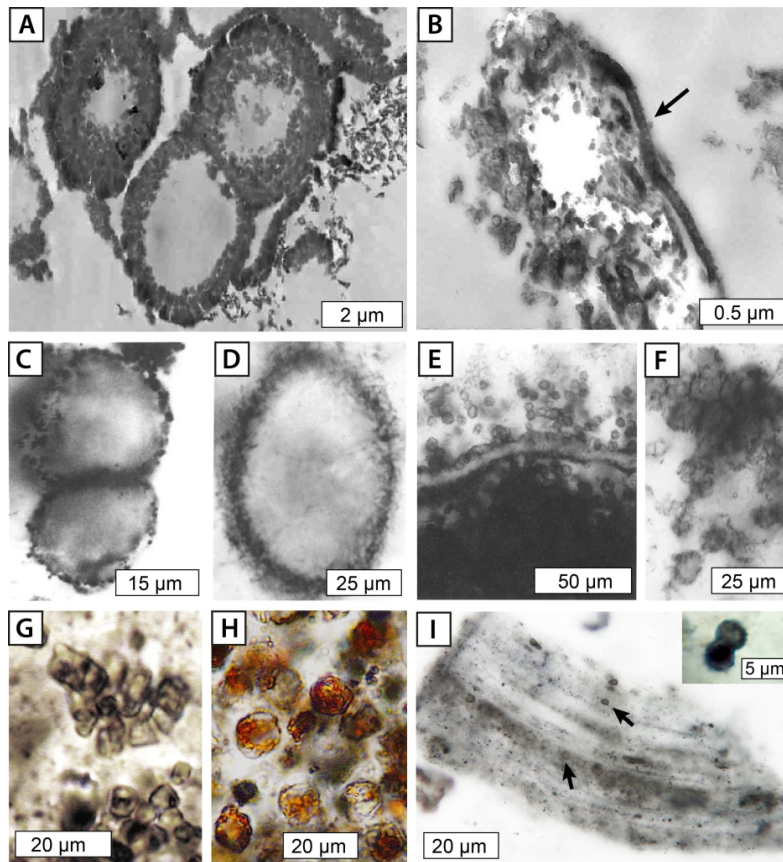
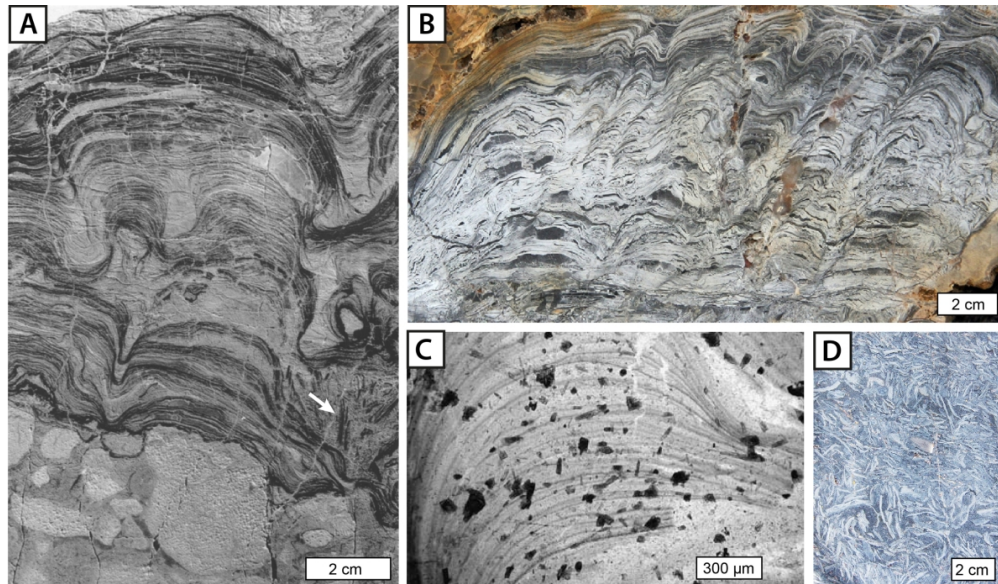


Fig. 9. Photomicrographs of proposed spheroidal microfossils from cherts of the Onverwacht Group. A and B) Transmission electron microscopy (TEM) images of cell-like objects with granular, in places detached walls (arrow) from the Hooggenoeg Formation. C and D) Large spheroids and ellipsoids from the Buck Reef Chert. E and F) Clusters of thin-walled spheroids from the Buck Reef Chert. G and H) Groups of spheroidal microstructures with rounded to angular walls from the Buck Reef Chert. I) Putative organic microspheres (arrows) from the Msauli Chert, which show features resembling cell division (small image in the upper right corner). Images (A-D) from Glikson *et al.* (2008); Images (C-F) from Walsh (1992); Images (G and H) from Kremer and Kazmierczak (2017); Image (I) courtesy of Andrew H. Knoll.





**Fig. 10.** Putative stromatolites and laminated silica crusts from the upper Onverwacht and Fig Tree Group. A) Polished slab showing morphologically diverse stromatolites overlying and draping the brecciated top of a komatiitic lava flow. Small basal domes successively grade into pseudocolumnar stromatolites with bridging laminations that are, in turn, overlain by low-relief domal laminations. Note the eroded stromatolite chips adjacent to the basal dome (arrow). B) Laminated silica crusts with inclined stromatolite-like columns and domes. C) Photomicrograph showing fine primary carbonaceous laminae with variable enrichment in secondary fine-grained tourmaline (dark minerals). D) Conglomerate of laminated silica chips interpreted as fragments of eroded stromatolites or sinter crusts. *Images (A and C) from Byerly and Palmer (1991), (B and D) from Lowe and Byerly (2018).*

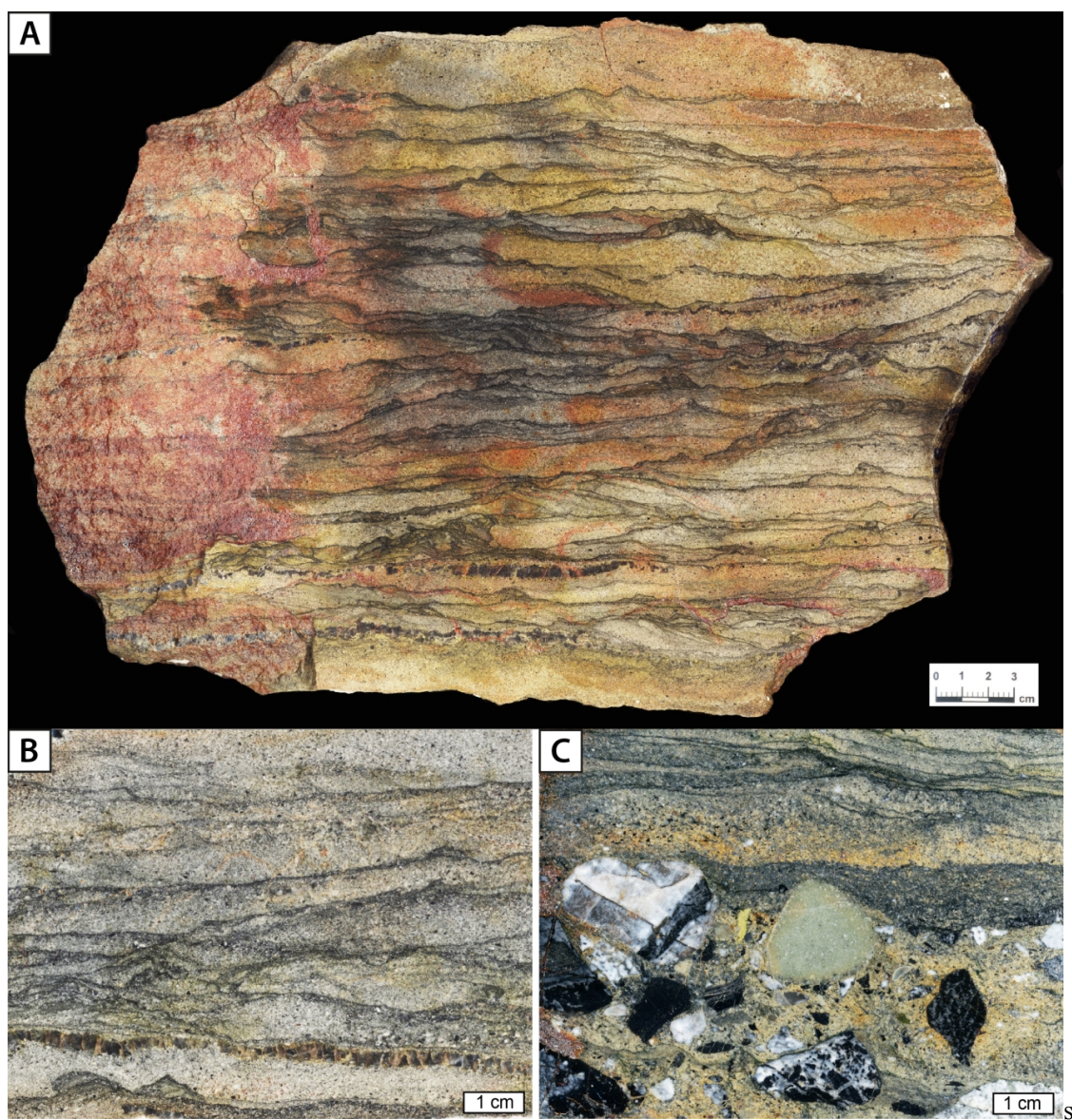


Fig. 11. Comparison of fossil microbial mats from tidal marine (A, B) and fluvial (C) deposits of the 3.22 Ga Moodies Group. A, B) Polished slab photographs of marine mats from the Saddleback Syncline showing densely spaced, crinkly carbonaceous laminations with small domes and tufts. The fossil mats are interbedded with medium- to coarse-grained sandstone and in places underlain by bedding-parallel chert lenses interpreted as silicified cavities. C) Terrestrial mats from the fluvial deposits of the Dycedale Syncline draping and onlapping interbedded clasts. Note that the preserved carbonaceous laminae are often thicker in comparison with the marine mats.



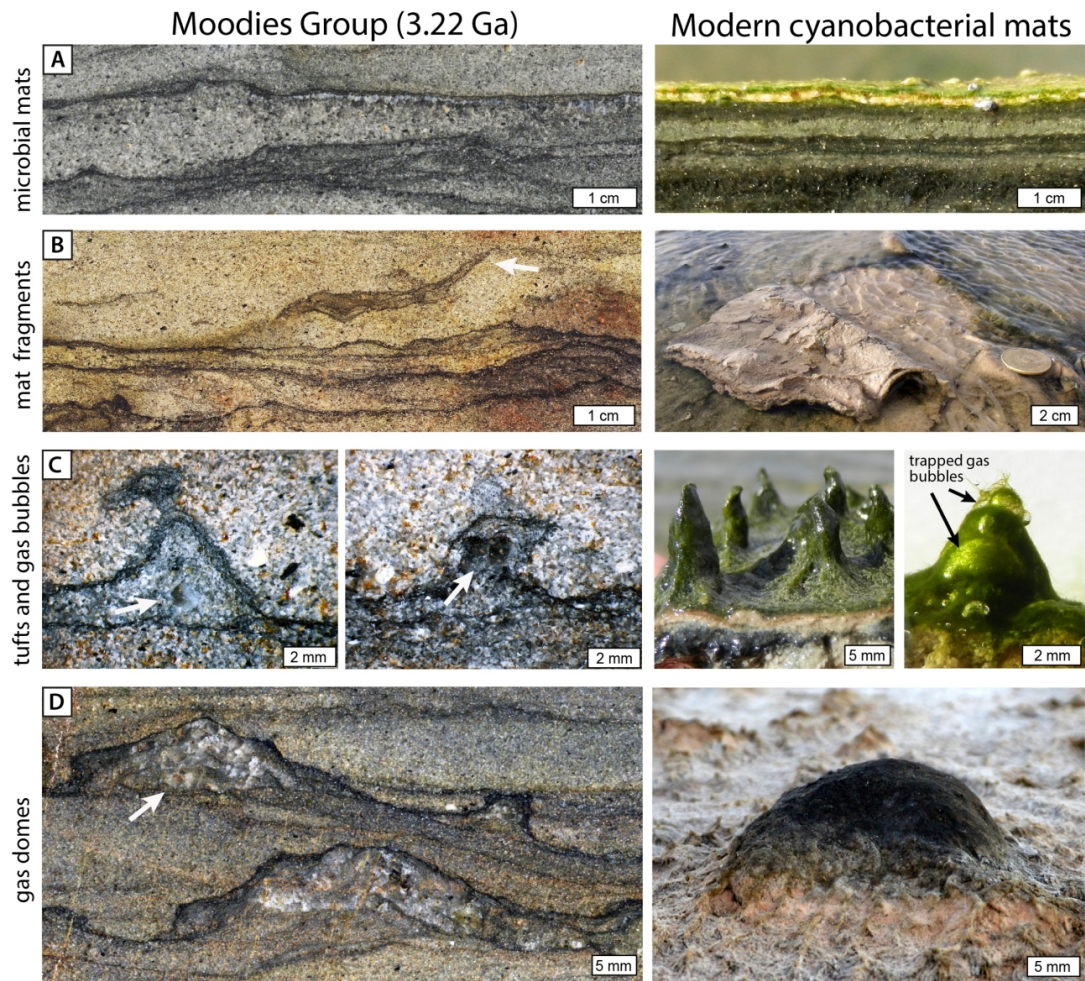


Fig. 12. Comparison of fossil intertidal microbial mats from the 3.22 Ga Moodies Group (left) with modern cyanobacterial mats from the tidal flats of Bahar Alouane, Tunisia (right). A) Crinkly carbonaceous mat laminations. B) Eroded mat fragment (arrow) and roll-up structure indicative for a cohesive consistency. C) Microbial tufts with now silicified cavities (arrows) interpreted as fossil gas bubbles, resembling trapped oxygen-rich bubbles in modern tufted mats. D) Silicified gas domes beneath the Moodies mats (arrow) and modern analogue of similar shape and size from Tunisia.



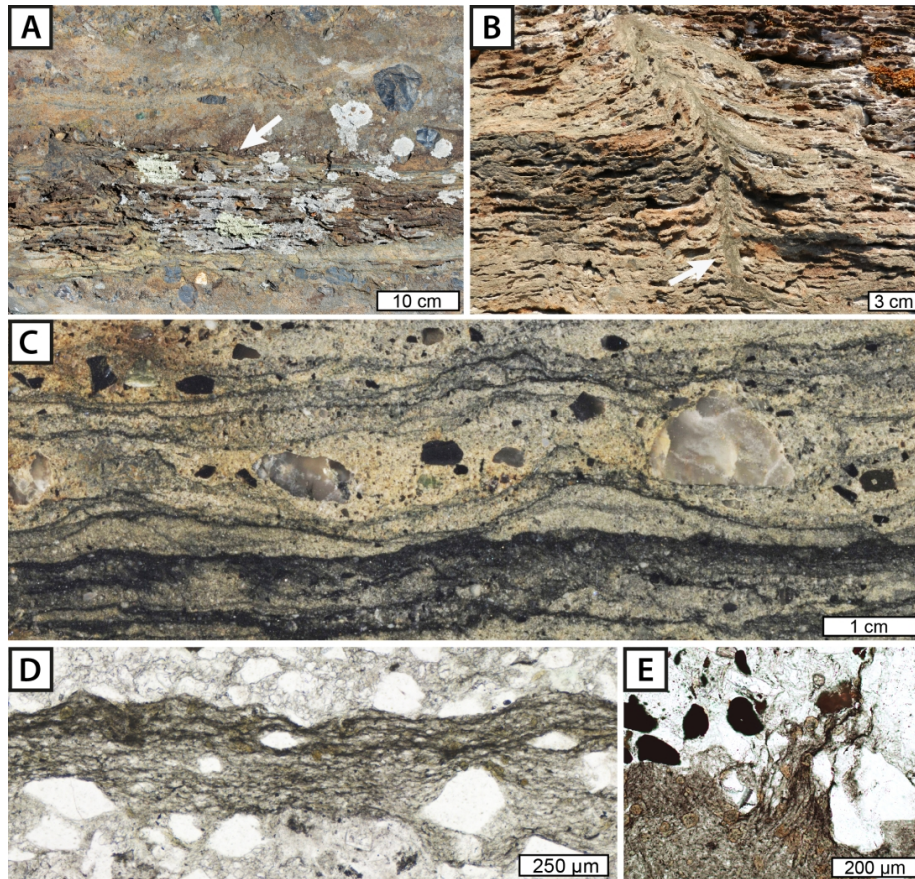


Fig. 13. Fossil terrestrial microbial mats from fluvial sandstones and conglomerates of the Moodies Group. A) Field photograph of the fluvial mats (arrow) interbedded with gravelly sandstones. B) Microbial mats disrupted and deformed by subvertical fluid-escape structure with well-defined central channel (arrow). C) Polished slab photograph with dark carbonaceous laminae of the fossil mats, draping former sedimentary surfaces and onlapping pebbles. D) Close-up view of the laminae, which show a dense meshwork of interwoven filamentous microstructures with trapped detrital grains. E) Filament-like microstructures in the upper, partially eroded part of the mat. *Images (A-E) from Homann et al. (2018).*

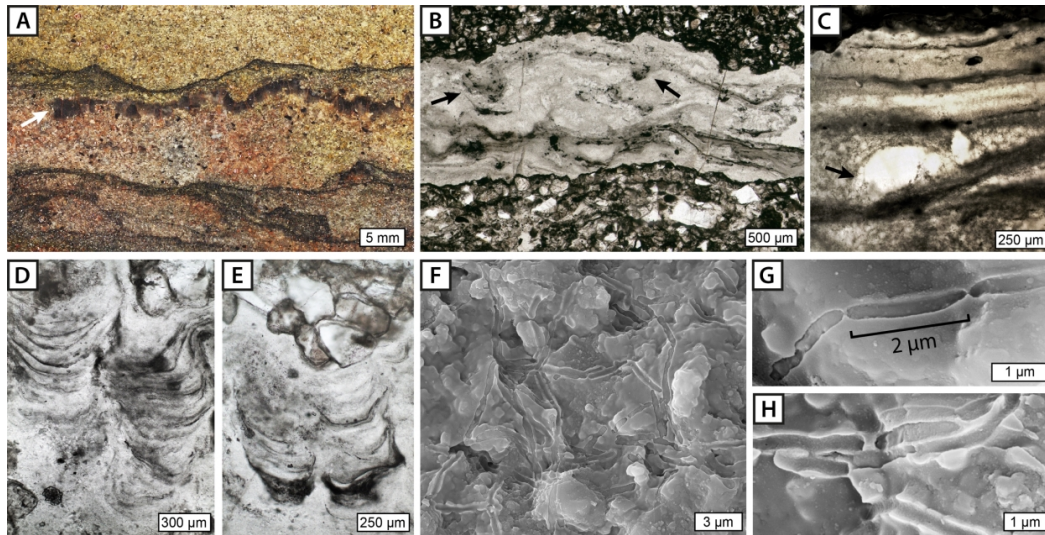


Fig. 14. Evidence for cavity-dwelling microbial life in the tidal deposits of the Moodies Group. A) Polished slab photograph showing silicified bedding-parallel cavity beneath fossil microbial mat (arrow). B) Photomicrograph of the silicified cavities with carbonaceous laminations, wisps, and pendant protrusions at the cavity ceiling (arrows). C) Carbonaceous laminae surrounding ovoid-shaped structure interpreted as trapped gas bubble (arrow). D and E) Close-up view of downward-facing columnar microstromatolites with preserved internal carbonaceous laminae. F) SEM image showing meshwork of filament molds embedded and permineralized in chert. G and H) Filamentous molds with regularly, spaced, rod-shaped segments of approximately similar length. *Images (B and D-H) from Homann et al. (2016).*

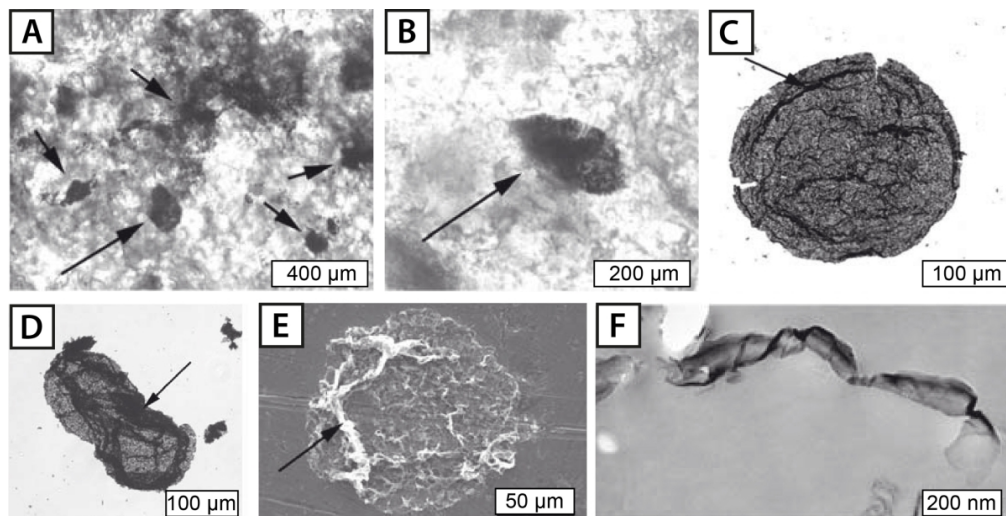


Fig. 15. Large organic-walled microfossils from the Moodies Group. A and B) Compressed spheroidal structures (arrows) in petrographic thin section. C and D) Microstructure extracted from the rock by acid maceration showing concentric folding (arrow in C) and collapse (arrow in D) of the wall. E) SEM image showing the folded, wrinkled and degraded texture of the wall (arrow). F) TEM image of ultrathin section showing homogenous ultrastructure of the torn and wrinkled 'cell' wall. *Images (A-F) from Javaux et al. (2010).*

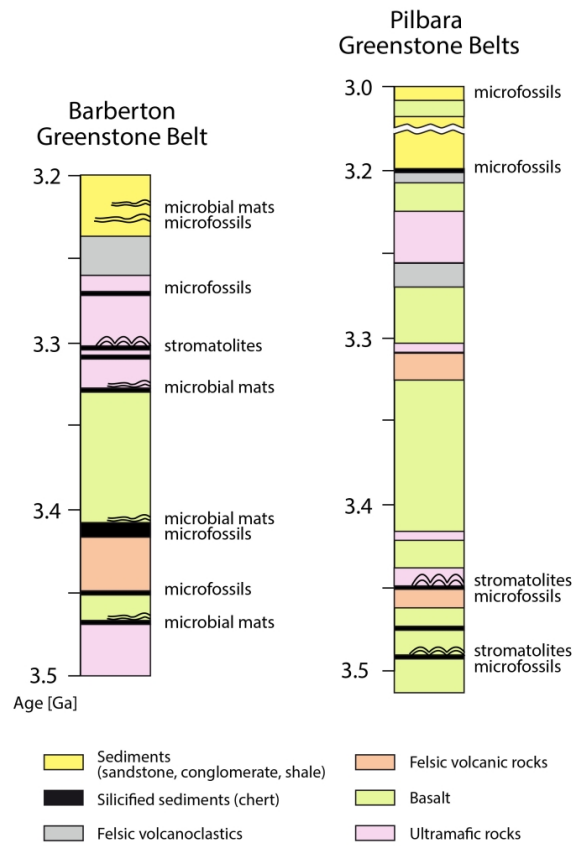


Fig. 15. Simplified stratigraphy and traces of early life in the Barberton Supergroup of South Africa in comparison with the Pilbara Supergroup of Western Australia.

**Table 1 | Claims for Paleoproterozoic Life in the Barberton Greenstone Belt, South Africa**

Age [Ma]	Lithostratigraphic Unit	Paleoenvironment	Morphological Evidence	Geochemical Evidence	Comments
~3220 <sup>1</sup>	<b>Mooides Group</b>	Tidal marine coastline	<b>Microbial mats:</b> densely-spaced carbonaceous laminae interbedded with tidal sandstones (Nothke et al., 2006; Heubeck 2009; Gamper et al., 2012), cohesive erosion-resistant behavior, distinct mat morphologies (planar, crinkly, tufted); fossil gas bubbles, shrinkage cracks, eroded and reworked mat fragments, mm- to cm-sized silicified gas domes, and widespread fluid-escape structures (Homann et al., 2015).	$Bulk\ \delta^{13}C_{org}$ : -33.9‰ to -21.3‰ (n=30) $Bulk\ \delta^{15}N$ : -0.7‰ to +3.1‰ (n=9) Raman $T_{max}$ : ~366°C	Well-established depositional, and petrographic context, widespread occurrence (15 km along strike), facies dependent mat morphology, combined with evidence for biogeochemical cycling of carbon and nitrogen strongly suggest a biogenic origin (Homann et al., 2018).
			<b>Cavity-dwelling microbial communities:</b> downward-growing microstromatolitic columns and carbonaceous laminae preserved in silicified cavities beneath the mats, fossil gas bubbles, interwoven filamentous molds (0.3–0.5 μm in diameter) with regularly spaced, rod-shaped segments interpreted as microfossils (Homann et al., 2016).	$In\ situ\ \delta^{13}C_{org}$ : -32.3‰ to -21.3‰ (n=12)	Well-established sedimentological and petrographic context and <i>in situ</i> carbon isotopes support the oldest evidence of cavity-dwelling microbial life.
		Shallow-marine deltaic?	<b>Organic-walled microfossils:</b> of carbonaceous composition preserved in shales and siltstones, spheroidal shape (up to 300 μm in diameter), cellular morphology and ultrastructure, occurrence in populations (Javaux et al., 2010; Burck, 2010).	$Bulk\ \delta^{13}C_{org}$ : -28.3‰ to -16.4‰ (n=22)	A promising sign for life, carbon isotopes would be more convincing if measured <i>in situ</i> on individual microfossils.
		Braided fluvial to supratidal	<b>Paleosols:</b> containing pedogenic carbonates, sulfates, and pyrite grains with biogenic overgrowth rims (Nabhan et al., 2016a, b).	$In\ situ\ \delta^{34}S_{C-DIF}$ : -25‰ and -20‰ (n=105) suggestive for microbial fractionation of sulfur	Detailed stratigraphic and petrographic context support Earth's oldest known signs for biogenic sulfur cycling on land.
		Fluvial, coastal braidedplain	<b>Microbial mats:</b> of carbonaceous composition (Homann et al., 2018), draping gravely sandstone beds and conglomerates of fluvial-alluvial origin (Heubeck and Lowe, 1994; Eriksson et al., 2006; Heubeck et al., 2016) associated with desiccation cracks, eroded mat fragments and fluid-escape structures.	$Bulk\ \delta^{13}C_{org}$ : -23.6‰ to -17.9‰ (n=36) $Bulk\ \delta^{15}N$ : +1.9‰ to +5.6‰ (n=10) Raman $T_{max}$ : ~363°C	Earth's earliest combined fossil and geochemical evidence for the microbial colonization of terrestrial habitats on the emergent continental landmass.
~3250	<b>Fig Tree Group</b> Sheba Fm.	Shallow-water to subaerial, evaporitic	<b>Stromatolites:</b> with tourmaline-rich, carbonaceous laminae preserved in cherts as laterally linked, low-relief domes (1–3 cm wide, 0.5–3 cm high) and compound domes or pseudocolumns of up to 10 cm height. (Byerly et al., 1986; Byerly and Palmer, 1991). Fragments of eroded stromatolites or sinter crusts (Lowe and Byerly 2015, 2018).	None, except carbonaceous composition	Widespread (>10 km along strike) and morphological diverse. Possibly Africa's oldest stromatolites, but more evidence needed.
3298 <sup>2</sup>	<b>Onverwacht Group</b> Mendon Fm. (M2c)			None, except carbonaceous microfossil walls	Possible life, but geological context and geochemistry needed to further support biogenic origin.
	Mendon Fm.* (previously named Swartkoppie Fm.)	?	<b>Possible microfossils:</b> lenticular [spindle-shaped] (30–70 μm in long axis) and spheroidal (5–50μm) shapes preserved in chert, occurrence as individuals or in clusters and chains, which might resemble remains of former colonies (Pflug 1966, 1967; Pflug et al., 1969). *Cherts were originally assigned to the Fig Tree Group.	None, except carbonaceous microfossil walls	
	Mendon Fm.*	?	<b>Possible microfossils:</b> spheroidal structures, ~19 μm in diameter (Barghoorn and Schopf, 1966; Schopf and Barghoorn, 1967).	None, except carbonaceous microfossil walls	Simple morphology, and no depositional context or geochemistry reported. Could likely be non-biological (Wacey, 2009)
	Mendon Fm. (M1c) (Msaufi Chert)	Shallow-marine to nearshore	<b>Possible microfossils:</b> spheroidal structures (1–4 μm in diameter) showing possible cell division (Knoll and Barghoorn, 1977).	None, except carbonaceous microfossil walls	Possible life, but hydrothermal fluids can mobilize and redistribute organic matter into spheroids (Knoll et al., 2016). High-resolution analysis needed to support biogenicity.



Age [Ma]	Lithostratigraphic Unit	Paleoenvironment	Morphological Evidence	Geochemical Evidence	Comments
3334 <sup>2</sup>	Kromberg Fm. (K3) (Josefsdal Chert)	Nearshore, possibly hydrothermal	<b>Microbial mats:</b> carbonaceous laminae (~10µm thick) in layered packets of 100–1000 µm thickness, eroded fragments of biofilms. (Westall et al., 2001; 2006, 2011; 2015). Putative rod-shaped microfossils are probably abiogenic (Altermann, 2001; Wacey 2009).	<i>Bulk</i> $\delta^{13}C_{org}$ : -26.8‰ and -22.7‰ (n=2)  <i>In situ</i> : $\delta^{13}C_{org}$ : -45‰ to -13‰ $\delta^{34}S$ : -24‰	Petrographic observations and geochemical signals support the biogenic origin.
3416 <sup>3</sup>	Kromberg Fm. (K1) (Buck Reef Chert)	shallow-marine	<b>Microbial mats:</b> fine carbonaceous laminae with different morphotypes, draping underlying sediments and detrital particles, filaments (1-1.5 µm in diameter), rolled-up fragments, carbonaceous grains (Walsh and Lowe, 1999; Tice and Lowe, 2004a, 2006a, b; Tice, 2009; Tice et al., 2011).  <b>Probable microfossils:</b> lenticular structures (13–135 µm long and 4.5–61 µm wide) with hollow center, interpreted as remnants of possibly planktonic microbes (Walsh, 1992; Oehler et al., 2017). Similar structures also occur in cherts of the Pilbara Craton.  <b>Possible microfossils:</b> filamentous structures (1.2–1.4 µm in diameter), sometimes interwoven clumps spheroidal structures (10–84 µm and 4.5–12.8 µm in diameter) (Walsh and Lowe, 1985; Walsh 1992, 2000)	<i>Bulk</i> $\delta^{13}C_{org}$ : -36.9‰ and -20.1‰ (n=19)  <i>In situ</i> $\delta^{13}C_{org}$ : -39.3‰ to -35.5‰ (n=8)  None, except carbonaceous composition	Widespread, well-documented, and morphological complex evidence for life.  Depositional context, morphological complexity, and narrow range of $\delta^{13}C_{org}$ values support a biological origin.  High-resolution petrographic and <i>in situ</i> carbon isotope analysis needed.
3416 <sup>3</sup>	Kromberg Fm. (K1c2) (Buck Reef Chert)	shallow-marine	<b>Possible microfossils:</b> spheroidal (3–12 µm in diameter) interpreted as remains of benthic-planktonic microbes, resembling coccolidal cyanobacteria (Kernerer and Kazmierczak, 2017).	<i>Bulk</i> $\delta^{13}C_{org}$ : -26.5‰ and -24.3‰ (n=2)	Morphologically simple structures with angular terminations. Nanoscale analysis and <i>in situ</i> geochemical data needed.
~3450	Kromberg Fm. and Hoogenoeg Fm.	Submarine pillow basalts	<b>Possible trace fossils:</b> filament-shaped and titanite-mineralized microtubes (4 µm in diameter and up to 200µm in length) in glassy pillow lava rims (Furnes et al., 2004). Similarly to microtubes from recent pillow lavas, but even their microbial origin is debated (Wacey et al., 2017).	<i>Bulk</i> $\delta^{13}C_{carb}$ : -16.4‰ to +3.9‰ <i>In situ</i> $\delta^{34}S_{Fe-CDT}$ : -40‰ to -3‰ from pyrite	Syn- and biogenicity questioned by Grosch and McLaughlin (2014) and Grosch et al. (2016), structures likely formed abiotically during post depositional contact metamorphism.
	Hoogenoeg Fm.	?	<b>Possible microfossils:</b> spheroidal and cup-shaped structures, 5–106 µm in diameter (Engel et al., 1968).	None, except carbonaceous composition	Probably of non-biological origin (Nagy and Nagy, 1969; Schopf and Walther, 1983).
3470 <sup>4</sup>	Hoogenoeg Fm. (H3c, H5c)	Seafloor, possibly hydrothermal	<b>Possible microfossils:</b> spheroidal structures (2–10 µm in diameter) with granular 'cell' walls interpreted as remnants of chemosynthetic microbes (Glikson et al., 2008). Morphological similarity to modern hyperthermophilic microbes.	None	Promising sign for life, but no geochemical data.
3472 <sup>5</sup>	Hoogenoeg Fm. Middle Marker (H1)	Shallow marine, associated with volcanic activity	<b>Microbial mats:</b> fine, crinkly to micro-tufted laminations, 'trapped' detrital sediment, wispy-like microstructures interpreted as eroded biofilm or mat fragments (Hickman-Lewis et al., 2018).	None, except carbonaceous composition and REE data	Carbon isotope data needed to further support biogenicity of the possibly most ancient trace of life in the BCB.

**Age Dates:** <sup>1</sup>Heubeck et al., 2013    <sup>2</sup>Byerly et al., 1999    <sup>3</sup>Kröner et al., 1991    <sup>4</sup>Byerly et al., 1999    <sup>5</sup>Armstrong et al., 1990